

Historical records from dated sediment cores reveal the multidecadal dynamic of the toxic dinoflagellate *Alexandrium minutum* in the Bay of Brest (France)

Klouch Khadidja ^{1,2}, Schmidt Sabine ³, Andrieux-Loyer Françoise ¹, Le Gac Mickael ¹, Hervio-Heath Dominique ⁴, Qui-Minet Zujaila Nohemi ¹, Quéré Julien ¹, Bigeard Estelle ², Guillou Laure ², Siano Raffaele ^{1,*}

¹ Ifremer, Centre de Brest, DYNECO PELAGOS, F-29280 Plouzané, France

² Sorbonne Universités, UPMC Univ. Paris 6, CNRS, Adaptation et Diversité en Milieu Marin (UMR 7144), équipe DIPO, Station Biologique de Roscoff, Place Georges Teissier, CS90074, 29688 Roscoff cedex, France

³ UMR5805 EPOC, Univ. Bordeaux, 33605 Pessac, France

⁴ Ifremer, RBE, SG2M, Laboratoire Santé, Environnement et Microbiologie, Plouzané, France

* Corresponding author : Raffaele Siano, Tel: +33 02 98 22 42 04; Fax: +33 02 98 22 45 48 ;
email address : raffaele.siano@ifremer.fr

Abstract :

The multiannual dynamic of the cyst-forming and toxic marine dinoflagellate *Alexandrium minutum* was studied over a time scale of about 150 years by a paleoecological approach based on ancient DNA (aDNA) quantification and cyst revivification data obtained from two dated sediment cores of the Bay of Brest (Brittany, France). The first genetic traces of the species presence in the study area dated back to 1873 ± 6. Specific aDNA could be quantified by a newly-developed real-time PCR assay in the upper core layers, in which the germination of the species (in up to 17–19 year-old sediments) was also obtained. In both cores studied, our quantitative paleogenetic data showed a statistically significant increasing trend in the abundance of *A. minutum* ITS1 rDNA copies over time, corroborating three decades of local plankton data that have documented an increasing trend in the species cell abundance. By comparison, paleogenetic data of the dinoflagellate *Scrippsiella donghaiensis* did not show a coherent trend between the cores studied, supporting the hypothesis of the existence of a species-specific dynamic of *A. minutum* in the study area. This work contributes to the development of paleoecological research, further showing its potential for biogeographical, ecological and evolutionary studies on marine microbes.

Keywords : paleoecology, ancient DNA, real-time PCR, Harmful Algal Blooms (HAB), dinoflagellates, coastal ecology

Introduction

Marine sediments are important resources for paleobiologists as they represent a valuable archive of past environmental communities. The resting stages of plankton, diatom frustules and spores, dinoflagellate cysts, foraminifera shells, and micro- and meso-zooplankton (rotifers, copepods, cladocerans, ciliates), as well as molecules such as sterols and pigments, can be accumulated and preserved in sediments. Their examination combined with a chronological analysis can provide ecological and environmental information about past communities (Liu *et al.* 2013; Ellegaard *et al.* 2013b). Benthic resting stages are derived from the rapid response of planktonic stages to unfavorable environmental conditions and are part of the life cycle of species. They are known to be powerful tracers of habitat changes because of their good preservation in sediment (Ellegaard *et al.* 2013a). In particular, phytoplankton resting stages have been widely used to reconstruct past environmental changes in temperature (de Vernal *et al.* 2005; Durantou *et al.* 2012; Weckström *et al.* 2006), salinity (Laird *et al.* 1996; Verleye *et al.* 2009; Mertens *et al.* 2012), productivity (Mertens *et al.* 2009; Pospelova *et al.* 2015), and eutrophication (Ellegaard *et al.* 2006; Zonneveld *et al.* 2012). Cultures derived from revived phytoplankton resting stages have been used to investigate the impact of environmental changes on the physiological performance of species (e.g. the dinoflagellate *Pentaparsodinium dalei*) in Koljö Fjord, Sweden (Ribeiro *et al.* 2013), or the genetic structure and diversity of populations of diatoms (*Skeletonema marinoi*) revived from sediments of Mariager Fjord, Denmark (Härnström *et al.* 2011).

The analysis of ancient DNA (aDNA) recovered from marine sediments is a complementary approach to the study of other biological remains in sediments that shows great potential. Several recent studies have demonstrated that plankton aDNA can be recovered from lacustrine and marine sediments, from the Holocene to the Pleistocene

(Coolen and Overmann 2007; Boere *et al.* 2011) and up to the Miocene (Panieri *et al.* 2010). Most of the DNA stored in marine sediments is believed to be extracellular, as it is protected from nuclease degradation by adsorbing to mineral and organic matrices (Pietramellara *et al.* 2009), but DNA may also originate from resting stages (Godhe *et al.* 2002, Erdner *et al.* 2010). Whatever its origin, this aDNA could be exploitable to study plankton ecological patterns over relatively long-term periods.

The long-term dynamics of marine protist species are usually deduced from multiannual time series, generally obtained from regular spatial-temporal coastal surveys carried out within the framework of monitoring network activities (e.g. Shuler *et al.* 2012; Hernández-Fariñas *et al.* 2014). Long-term series generally focus on potentially toxic species, such as *Alexandrium* spp. (e.g. Touzet *et al.* 2011; Abdenadher *et al.* 2012; Martin *et al.* 2014; Anderson *et al.* 2014; Bazzoni *et al.* 2015). However, most of these historical datasets are relatively short, covering only a few decades (<50 years), and are compromised by the limitations of identifying plankton species in routine optical microscopic analyses. Early information on past communities and species before the implementation of monitoring networks is therefore lacking. Paleoecological data could be an alternative to fill the gaps in the historical information about long-term protist community trends. Previous paleoecological analyses have shown multidecadal shifts and trends for diatom (Lundholm *et al.* 2010) and dinoflagellate species (Ribeiro *et al.* 2011), as well as for plankton communities (Mousing *et al.* 2013) using fossilized remains. aDNA has also been used to describe plankton succession dynamics (e.g. Bissett *et al.* 2005; Epp *et al.* 2010; Theroux *et al.* 2010; Stoof-Leichsenring *et al.* 2012, and Lejzerowicz *et al.* 2013 in old sediment (up to 32 000 years)) and to investigate the response of paleo-planktonic communities to past environmental changes (Coolen *et al.* 2013; Hou *et al.* 2014).

Alexandrium minutum is a cyst-forming dinoflagellate (Alveolata), responsible for several Harmful Algal Blooms (HAB) associated with toxin production causing Paralytic Shellfish Poisoning (PSP). Since its first detection in Alexandria harbor, Egypt (Halim 1960), this species has been detected in several areas: southern Australia (Hallegraeff *et al.* 1988), Ireland (Gross 1989), northern France (Belin 1993), the Mediterranean (Honsell 1993), Spain (Franco *et al.* 1994), the North Sea (Nehring 1998; Elbrachter 1999; Hansen *et al.* 2003), Taiwan (Hwang *et al.* 2000), New Zealand (Chang *et al.* 1999), Sweden (Persson *et al.* 2000), India (Godhe *et al.* 2001) and Malaysia (Usup *et al.* 2002). *Alexandrium minutum* is officially listed as an invasive species in Europe (<http://www.europe-aliens.org>) and is considered cryptogenic as its geographical origin is unknown (Gómez 2008; Katsanevakis *et al.* 2014). Phylogeographic analyses by Lilly *et al.* (2005) and McCauley *et al.* (2009) have shown that *A. minutum* populations can be clearly differentiated into two major clades: the global clade (containing samples from Europe and Australia) and the Pacific clade (containing samples from New Zealand and Taiwan). Yet, it remains quite challenging to determine whether recent *A. minutum* populations were introduced through natural or human-assisted pathways. In the Bay of Brest (Brittany, France), *A. minutum* has been detected since 1990 by the monitoring network REPHY (*REseau de surveillance et d'observation du PHYtoplankton et des PHYcotoxines*) (http://envlit.ifremer.fr/surveillance/phytoplankton_phycotoxines/presentation) but its abundance was rather low (<2000 cells L⁻¹) until recent years when it increased significantly in the area. In July 2012, it reached a record concentration of around 42 million cells L⁻¹. This exceptional bloom induced a cascading effect: toxin accumulation in shellfish, closure of aquaculture activities and economic losses, leading to the Bay of Brest being classified as a new high-risk zone for toxic blooms of *A. minutum* (Chapelle *et al.* 2015).

The objective of this work was to contribute to studies on marine microbial paleoecology and long-term dynamics of HAB dinoflagellate species by collecting historical information on *A. minutum* in the Bay of Brest. More specifically, cyst germination experiments were used to detect the viability of the species in ancient sediments and a newly-developed real-time PCR assay on aDNA was employed to try to reconstruct the multidecadal dynamic of the species in the area. In order to evaluate the specificity of the *A. minutum* ecological pattern, paleogenetic data obtained for *Scrippsiella donghaiensis* were analyzed, as an example of a different, non-toxic, cyst-forming dinoflagellate species of this area. In parallel, plankton-monitoring data collected since 1990 in the Bay of Brest were analyzed in order to verify whether the dynamic of *A. minutum* in the water column were consistent with the results obtained by paleogenetic data during the overlapping period of the two data series.

Materials and methods

Study sites and phytoplankton monitoring

The Elorn and Daoulas estuaries are located in the Bay of Brest (Brittany, North Atlantic, north-west coast of France). They are both situated near areas of intensive agriculture, domestic waste and industrial discharges, which all contribute to the substantial nutrient supply of these estuaries. Since 1950, coastal ecosystems of the bay have experienced a large increase in their nutrient supply caused by the development of anthropogenic activities. More recently, the ban on washing powders containing orthophosphates has resulted in a decrease in the phosphorous supply leading to a significant imbalance in the N/P ratio (Guillaud and Bouriel 2007). This environmental change has been associated with variations in phytoplankton communities over time, such as an increase in phytoplankton biomass and in

the intensity and frequency of HABs (Guillaud and Bouriel 2007). The REPHY monitoring network has been recording occurrences of phytoplankton species in French coastal ecosystems since 1984. In the Bay of Brest, monitoring is carried out at three sampling stations: *Le Passage* in the Elorn River estuary, from 1990 to 2004 and then from 2012 to date, *Lanveoc*, from 1993 to date, and *Daoulas*, which became the third spot point in the area after the impressive toxic bloom event of *A. minutum* in July 2012 (42×10^6 cells L⁻¹) (Fig. 1). This last station is monitored during the summer period only (May-August), which corresponds to the highest productivity period when toxic blooms are most likely to occur. Fortnightly analyses of lugol-fixed samples are carried out using light microscopy. The estimations of *A. minutum* abundance are performed at a specific level, sometimes only during the occurrence of species blooms or high-risk periods. The abundance of non-toxic species is not monitored regularly at all stations and sometimes not at the species level. This is the case for the taxon *Scrippsiella* spp., which, in the case of REPHY monitoring, can include species of other dinoflagellate genera (*Ensiculifera*, *Pentaparsodinium*, *Bysmatrum*) that cannot be distinguished in routine light microscopy analyses by phytoplankton observers. In this study, only samples with non-zero values corresponding to abundances ≥ 100 cells L⁻¹, which is the threshold abundance limit of species detection in the REPHY phytoplankton analysis procedures, were considered and analyzed.

Core sampling and processing

Sediment cores were collected on 11th December 2012 at station EE of the Elorn River Estuary (48°23'46.79''N 4°23'2.01''W), and on 21st May 2014 at station DE (48°20'46.6''N 4°17'41.20''W) of the Daoulas Estuary (Fig. 1). The sampling sites were selected on the basis of their suitable environmental characteristics for paleoecological analysis (calm

hydrodynamics favorable for regular sedimentation (Rawlence *et al.* 2014)) and their proximity to the REPHY stations. Three cores were collected at station EE for genetic (31 cm) germination (25 cm) and dating (29 cm) analyses, respectively. Two cores were collected at DE, one (58 cm) for genetic and dating analyses and the other (59 cm) for cyst germination experiments. Visual inspection revealed no differences in the structure of the cores from the same sampling site. The EE cores were collected by divers at 12 m depth using hand-driven transparent Plexiglas tubes, 9.5 cm in diameter and 60 cm in length. The DE cores were collected at 3 m depth with a corer released from the boat. Immediately after sampling, the sediment cores were delicately extruded from the Plexiglas tubes and then sliced into 1-cm layers. Sterile new equipment was used to slice each layer sample. For DNA and cyst germination analyses, to avoid contamination by smearing between the layers during the core extraction, only the inner part of each slice was sampled, using sterile 6-cm-diameter Petri dishes. The sediment samples for genetic analyses (about 10 g) were preserved in plastic 50-mL cryotubes. The tubes were frozen in liquid nitrogen and then stored in a -80°C freezer until further analyses. The sediment samples for cyst germination were collected in 50-mL tubes and stored in the dark at 4°C. Finally, sediment aliquots for dating were stored in plastic bags until radionuclide analyses.

²¹⁰Pb and ¹³⁷Cs dating

The chronological framework of the sediment cores was determined based on ²¹⁰Pb_{xs} and ¹³⁷Cs as previously performed in Schmidt *et al.* (2007) and Andresen *et al.* (2014). ²¹⁰Pb (T_{1/2} = 22.3 years) is a naturally occurring radionuclide delivered continuously to the landscape by atmospheric fallouts (Saari *et al.* 2010). This atmospherically-derived ²¹⁰Pb, readily scavenged by sediment, is referred to as ²¹⁰Pb in excess (²¹⁰Pb_{xs}) of that found within particles

due to the decay of its parent isotope, ^{226}Ra . On the contrary, ^{137}Cs ($T_{1/2} = 30$ years) is an artificial radionuclide: its occurrence in the environment is primarily the result of the nuclear weapon test fallout in the early sixties and the Chernobyl accident in Europe in 1986 of well-known pulse inputs (Avşar *et al.* 2015). In the laboratory, water content was determined by weighing the sediment samples before and after freeze drying, and Dry Bulk Density (DBD) was subsequently calculated, assuming a mineral density of 2.65 g cm^{-3} . Following this procedure, ^{210}Pb , ^{226}Ra and ^{137}Cs activities were measured using a very low background, high-efficiency, well-shaped γ detector equipped with a Cryo-Cycle (CANBERRA) (Schmidt and de Deckker 2015). The γ detector was calibrated using certified reference materials from IAEA (RGU-1; RGTh; SOIL-6). Activities were expressed in mBq g^{-1} and errors were based on 1 SD counting statistics. Excess ^{210}Pb ($^{210}\text{Pb}_{\text{xs}}$) activities were calculated by subtracting the activity supported by its parent isotope, ^{226}Ra , from the total ^{210}Pb activity in the sediment.

Cyst germination experiments and strain identification

Cyst germination experiments were performed similarly to previous paleoecological studies on diatoms (Härnström *et al.* 2010) and dinoflagellates (Miyazono *et al.* 2012). Sediment samples ($\sim 5 \text{ cm}^3$) were added to filtered seawater and placed in an ultrasonic bath for 6 min to separate dinoflagellate cysts from inorganic particles. The sediments were sieved with filtered seawater through a $100\text{-}\mu\text{m}$ onto a $20\text{-}\mu\text{m}$ sieve to separate the sediment size fraction containing the majority of dinoflagellate cysts. Different media (F/2, site-specific seawater, K, K/2) and temperature (16 and 18°C) conditions were tested to optimize cyst germination. Irradiance ($60 \mu\text{mol photons m}^{-2} \text{ s}^{-1}$) and photoperiod (12 h:12 h) were kept constant during this optimization. Finally, the combination of 16°C and K medium (Keller *et al.* 1987) was retained. A few drops of the $20\text{-}100 \mu\text{m}$ fraction were distributed onto a 12-well plastic plate

containing K medium (2 mL per well). The plates were placed in a culture room at 16°C, under an irradiance of 60 $\mu\text{mol photons m}^{-2} \text{s}^{-1}$ and a light:dark cycle of 12 h:12 h. The plates were examined for vegetative cell germination once to three times per week using an inverted microscope (Zeiss Axiovert 135). *Alexandrium minutum* cells were identified by light microscopy, but we failed to establish monoclonal strains in culture. For *Scrippsiella* spp., clonal cultures were established from different sediment layers of both the EE and DE cores. A total of 65 strains of *Scrippsiella* spp. were finally obtained from 12 and 6 sediment layers of the EE and DE cores, respectively. The cultured strains were identified genetically. DNA was extracted from the strain cultures using the DNeasy plant mini kit (QIAGEN, Germany) following the manufacturer's instructions. The LSU rDNA region was amplified by PCR using dinoflagellate-specific primers (Ldino6, Ldino1) from Probert *et al.* (2014) and the following PCR program: 35 cycles composed of an initial denaturation at 95°C for 2 min, a denaturation at 95°C for 30 sec, a hybridization at 56°C for 30 sec, an elongation at 72°C for 1 min and a final elongation at 72°C for 5 min. After purification by the QIAquick PCR purification kit (QIAGEN, Germany), the PCR products were sent to GATC Biotech (<http://www.gatcbiotech.com/en/products/sanger-services>) for Sanger sequencing. All sequences were deposited in GenBank and 32 strain cultures (the remaining 33 strains were lost) are available at the Roscoff Culture Collection (RCC: <http://roscoff-culture-collection.org/>).

Genetic analyses of sediment samples

DNA extraction and quantification – Genetic analyses were carried out considering the specific precautions that should be taken when working with aDNA in order to avoid cross-contamination between samples and contamination with modern DNA (Gilbert *et al.* 2005).

Total DNA was extracted from 5-7 g of sediment material from each layer of the EE (31 samples) and the DE (58 samples) cores, using the PowerMax soil isolation kit (Mbio Laboratories Inc., Carlsbad, California, USA), following the manufacturer's instructions. DNA extracts were immediately stored at -80°C. DNA samples were quantified by absorbance measurements using a Take3 trio microplate reader (BioTek, Winooski, Vermont, USA) on 3 µL of DNA extract, and sterile water was used as a blank. DNA quality was checked by the 260/280 nm ratio to ensure that no contamination by proteins or other components had occurred during DNA extraction. For DNA concentration analyses, in order to determine whether a significant change had occurred in DNA concentrations and, if so, to estimate the change-point in DNA concentration across the sediment core layers, the Change-Point-Method (CPM) was applied on the total DNA concentration data along the DE and EE cores. This test is generally used to detect changes in the mean value in a data series (Taylor 2000).

Primer design and specificity – Specific primers for the amplification of *Alexandrium minutum* (synonym of *Alexandrium lusitanicum*) from genomic rDNA samples are available in the literature (Penna *et al.* 2010) but they generate longer amplicons (> 150 bp) than required (50-150 bp) for optimal real-time PCR efficiency. To optimize amplification success in aDNA, the use of short amplicons (ca. 100 bp) is recommended (Coolen *et al.* 2013). Therefore, new primer sets for specific real-time PCR targeting the ITS1 rDNA region were designed for the two target species in this study, *A. minutum* and *S. donghaiensis*. *Scrippsiella donghaiensis* was chosen as the second target species in the light of the successful germination analyses in old sediments and given its monophyletic separation in ITS topologies within the genus *Scrippsiella* (Gu *et al.* 2008), which enables a better specific primer design. Its

presence in northern European waters (i.e. Sweden) (Gu *et al.* 2008) makes *S. donghaiensis* an interesting model to compare with potential invasive species in the North Atlantic. A total of 176 ITS rDNA sequences of *A. minutum* and other *Alexandrium* species and a total of 59 ITS rDNA sequences of *S. donghaiensis* and other *Scrippsiella* species were downloaded from GenBank and aligned using Bioedit software (version 7.0.9.0). The primer sets were designed to target a fragment of 100-110 bp (using Primer3 software (<http://primer3.wi.mit.edu/>, Rozen and Skaletsk 2000)) (Table 1). The primers were analyzed for self/hetero-complementarities and secondary structure using OligoAnalyzer 3.1 software (<http://eu.idtdna.com/calc/analyzer>). Primer specificity was checked 1) *in silico*, by visual inspection of an alignment of ITS sequences, 2) *in silico*, using the Primer Blast tool (<http://www.ncbi.nlm.nih.gov/tools/primer-blast/>) and 3) in the laboratory, by conventional PCR using DNA from positive (*A. minutum* (3 strains) and *S. donghaiensis* (14 strains)) and negative (9 dinoflagellate species for a total of 27 strains) controls (see Supplementary Tables 1-4). The PCR mixture was identical for the two species except for the concentrations of the reverse and forward primers: 0.3 μ M for *A. minutum* and 0.5 μ M for *S. donghaiensis*, 1.25 u of GoTaq Polymerase, 2 mM of MgCl₂, 0.2 mM of dNTPs, 1X of GoTaq Flexi buffer, 2 μ L of DNA template and sterile water. The PCR conditions for *A. minutum* were as follows: an initial denaturation step at 95°C for 2 min, 35 cycles at 95°C for 30 sec, 62°C for 30 sec, 72°C for 30 sec and a final elongation step at 72°C for 2 min. For *S. donghaiensis*, the cycling program consisted of an initial denaturation step at 95°C for 5 min, 35 cycles at 95°C for 1 sec, 61°C for 45 sec, 72°C for 1 min and a final elongation step at 72°C for 7 min. The PCR products were loaded onto 1.5% agarose gel to confirm the presence of fragments of the expected length (100 bp for *A. minutum* and 110 bp for *S. donghaiensis*) and the absence of non-specific bands.

ITS1 rDNA cloning and standard curve construction – ITS1 rDNA PCR products of *Alexandrium minutum* (strain RCC 1490) and *Scrippsiella donghaiensis* (RCC 3047) were cloned separately into plasmids (pCR 4), then chemically transformed into *Escherichia coli* using a TOPO TA cloning kit (Invitrogen, USA) following the manufacturer's instructions. Several clones were obtained but only one clone of each species was retained for analysis. Plasmid DNA was isolated using the NucleoSpin Plasmid/Plasmid (NoLid) then linearized with a restriction enzyme "Not I". The plasmid was checked on a 1% agarose gel. Standard curves for real-time PCR (serially diluted plasmids containing the ITS1 rDNA fragment of *A. minutum* or *S. donghaiensis*) were constructed from the linearized plasmid DNA previously isolated. Plasmid DNA concentration was measured using a Quant-iT PicoGreen dsDNA quantification kit (Invitrogen, USA) and an FLX 80 fluorescence reader (BioTek, USA) according to the manufacturer's instructions. Quantification was performed using lambda DNA standards provided in the kit ranging from 2.5 to 1000 pg μL^{-1} . Plasmid concentration ($\text{ng } \mu\text{L}^{-1}$) was converted into (copy number μL^{-1}) according to the following equation:

$$\text{Number of copies per microlitre} = (\text{DNA concentration (ng L}^{-1}\text{)} / [660 \times (\text{plasmid size} + \text{insert size}) \times 10^9 \text{ (ng mol}^{-1}\text{)}]) \times 6.022 \times 10^{23} \text{ (molecules)}$$

For each target species, a standard curve was constructed with 10-fold serial dilutions of the linearized plasmid containing the ITS1 rDNA sequence of the species. Standard curves ranged from 10^6 to 10 copies μL^{-1} for *A. minutum* and from 10^5 to 10 copies μL^{-1} for *S. donghaiensis*.

Real-time PCR – Real-time PCR reactions were performed using the iTaq Universal SYBR Green supermix kit (Bio-Rad, USA) in a final volume of 20 μL . For *A. minutum* detection, the reaction mixture was composed of 10 μL of SYBR Green supermix (1X) containing (dNTPs,

iTaq DNA polymerase, MgCl₂, SYBR Green I), 0.3 μM of the forward primer (Am_48F), 0.2 μM of the reverse primer (Am_148R), sterile water and 2 μL of sample DNA template (variable concentration between 2.42 and 34.30 ng μL⁻¹). The experiments were conducted in 96-well plates containing the standard curve dilutions in duplicate, the target samples and the negative controls composed of water instead of DNA that were both analyzed in triplicate. The plates were loaded onto a Stratagene Mxpro3000P (Agilent Technologies, USA) thermal cycler with the following cycling conditions: 1 cycle at 95°C for 5 min followed by 40 cycles at 95°C for 5 sec and 62°C for 30 sec. A melting curve analysis was added at the end of each run to ensure specific *A. minutum* amplification. The optimal annealing temperature of 62°C was initially determined in conventional PCR. To determine the optimal primer concentration, 9 different combinations (forward/reverse), ranging from 0.1 μM to 0.3 μM, were tested on 3 dilutions of the standard curve (10⁶, 10³, 10 copies μL⁻¹). The primer combination that yielded the lowest threshold cycle value (Ct) and maximum real-time efficiency (Am_48F; 0.3 μM, Am_148R; 0.2 μM) was retained for further analysis. The real-time PCR mixture for *S. donghaiensis* detection was identical, except for the primer concentrations; 0.2 μM for the forward and reverse primer (SD_357F /SD_468R). The annealing temperature was determined at 61°C. The cycling conditions were: 1 cycle at 95°C for 5 min followed by 40 cycles at 95°C for 30 sec, 61°C for 30 sec and 72°C for 30 sec, and a final cycle at 95°C for 1 min followed by a melting curve analysis. The reaction efficiency was estimated by the equation $E = 10^{(1/b)} - 1$, where b is the slope of the standard curve. DNA amplifications of target species were considered positive if more than one out of the three replicates tested per sample was positive. The Limit Of Quantification (LOQ) was set at 10 copies per real-time PCR well, which was the smallest quantity of linear plasmid DNA of the standard curves for each real-time PCR assay. Concentrations of *A. minutum* or *S. donghaiensis* in each sediment

layer were expressed (assuming a 100% DNA extraction efficiency) in terms of copy number per gram of wet sediment, using the following formula:

$$\text{Copy number g}^{-1} = \text{copy number } \mu\text{L}^{-1} \times \text{DNA extraction volume } (\mu\text{L}) / \text{sediment wet weight (g)}$$

Sanger sequencing of Alexandrium minutum amplicons from sediment layers – In order to confirm the presence of *A. minutum* in sediment layers for which the real-time PCR amplifications were below the LOQ, amplicons resulting from a semi-nested PCR amplification of the DNA extract of the corresponding sediment layers were sequenced. The semi-nested PCR assays were carried out only for *A. minutum* as this was the major target species of our study. After the first amplification using designed primers for real-time PCR (Am_48F/Am_148R) (100 bp), 2 μL of the amplified material was used for the second PCR round performed with a new forward primer (Am_55F) and the same reverse primer (Am_148R) of the first PCR step (Table 1). Both PCR reaction mixtures were carried out in a final volume of 20 μL , using 2 μL of DNA template, 1X of GoTaq Flexi buffer, 2 mM of MgCl_2 , 0.2 mM of dNTP, 0.5 mM of each primer, 1.25 u of GoTaq polymerase (Promega) and sterile water. The PCR were performed in a PeqStar (OZYME) thermocycler with the following conditions: 1 cycle at 95°C for 2 min followed by 30 cycles at 95°C for 30 sec, 61°C for 30 sec, 72°C for 30 sec and a final cycle at 72°C for 2 min. PCR products were purified using the Nucleospin Gel PCR clean-up kit (Machery-Nagel, Germany) following the manufacturer's instructions, checked on an agarose gel. This semi-nested PCR procedure yielded an amplicon of 93 bp and a sufficient *A. minutum* DNA concentration for Sanger sequencing. Amplification products were sent to GATC Biotech (<http://www.gatcbiotech.com/en/products/sanger-services/>, Germany) for sequencing. The

resulting sequences were identified by BLAST and aligned in Bioedit with other *A. minutum* ITS1 rDNA sequences available in GenBank (<http://www.ncbi.nlm.nih.gov/genbank/>) (Table 2).

Statistical analyses on data series

In order to depict trends in the abundance of target species, the moving averages of real-time PCR data (copy number g^{-1} sediment) were calculated. This method is usually used to calculate long-term trends or cycles from time series data, smoothing out short-term fluctuations in a dataset, and has been used in paleoecological studies (e.g. Yu and Berglund 2007). The moving average of the *A. minutum* and *S. donghaiensis* genetic data series (copy number g^{-1} sediment) was calculated with a three-sample interval, meaning that an averaged value of the copy number g^{-1} was calculated for every three consecutive data (e.g. average of layers (1,2,3), average of layers: (2,3,4), etc.). These averaged values were used to produce the curves in Figure 3 representing the trend of the quantitative genetic data obtained for our studied species in the sediment samples. In addition, the Mann-Kendall trend test was performed on the real-time PCR data (copy number g^{-1} sediment) and the plankton data (cells L^{-1}) across the overlapping periods of the series (from 1989-2014) to detect statistically significant trends. The test was applied using the *Kendall* package in R software version 3.2.3 (R Core Team, 2015). The Mann-Kendall trend test is a non-parametric test for monotonic trends, which is typically used to detect whether there is a significant increasing or decreasing trend in a time series (Yue *et al.* 2002). In this test, the initial assumption is the null hypothesis (H_0), which assumes that there is no trend in the data series over time. The alternative hypothesis (H_1) is that there is a significant trend (increasing or decreasing) over time. The significance level of the test was set at $\alpha = 0.05$. If the p value < 0.05 , the H_0 is

rejected, meaning that there is a significant trend in the time series. Kendall's tau (τ) is a value between -1 and 1 that indicates the direction of the trend over time. An increasing trend is indicated by $\tau > 0$ and a decreasing one by $\tau < 0$.

Results

Sediment chronology

In the DE core, ^{210}Pb in excess activity ranged from 45 mBq g^{-1} in the uppermost sediment layers to $<1 \text{ mBq g}^{-1}$ at 58 cm (Fig. 2). There was a general trend of an exponential decrease in $^{210}\text{Pb}_{\text{xs}}$ as expected due to the decay of the unsupported ^{210}Pb . The $^{210}\text{Pb}_{\text{xs}}$ profile in the EE core showed the same trend: due to the shorter length of the sediment core, levels in which $^{210}\text{Pb}_{\text{xs}}$ became negligible were not reached. In both cores, the $^{210}\text{Pb}_{\text{xs}}$ decrease presented some irregularities. This could be related to temporary changes in sedimentation intensity, which justified the use of the CSR (constant rate of supply) model for dating (Fig. 2). The 31 cm-long EE core encompassed the last 72 years (from 1939 ± 2 to 2011 ± 1), whereas the DE core covered > 100 years (from 1866 ± 7 to 2013 ± 1). The sedimentary profile of ^{137}Cs in the two cores presented the expected shape with two peaks (nuclear weapon test fallout and Chernobyl) in the deepest layers. In the DE core, ^{137}Cs disappeared rapidly to negligible levels below the deepest peak. The EE core was too short to evaluate ^{137}Cs disappearance; however, the expected peak of the second atmospheric fallout was observed. In general, the sedimentary ^{137}Cs peaks in the two cores mimicked the atmospheric fallout rather well, validating the ^{210}Pb chronology (Fig. 2).

Germination experiments

Successful germinations were observed in both EE and DE cores (Table 3). Germinated cells belonged primarily to dinoflagellates (up to 17 cm (1978 ± 2) for EE and 20 cm (1981 ± 2) for DE) and diatoms (up to 11 cm (1991 ± 1) for EE and 13 cm (1995 ± 2) for DE). For the EE core, *S. donghaiensis* germinated predominantly along the core up to 17 cm (1978 ± 2) while cells of *A. minutum* were observed up to 7 cm (1999 ± 1). For DE, *S. donghaiensis* cells were observed up to 20 cm (1981 ± 2) and *A. minutum* was detected up to 13 cm (1995 ± 2) (see dotted line in Figure 3). Germinated diatom species belonged to *Skeletonema* spp., *Chaetoceros* spp., *Thalassiosira* spp., *Nitzschia* spp., *Lithodesmium* spp., *Paralia* spp., and *Asteromphalus* spp. Other autotrophic (*Peridinium quinquecorne*, *Gymnodinium* spp.) and heterotrophic (*Proto-peridinium* spp.) dinoflagellates were recorded along the two cores.

Molecular analyses

Total DNA concentrations extracted from the sediments ranged from 2.42 to 34.30 ng μL^{-1} for EE and from 3.46 to 26.70 ng μL^{-1} for DE. According to the 260/280 nm ratios, the DNA extracts were of sufficient yield and purity to conduct amplification analyses. A decreasing trend in total DNA concentration was observed from the top to the bottom of both EE and DE cores (see Supplementary Figure 1), with higher concentrations found in the first sediment layers of both cores. At 9 cm (10.84 ng μL^{-1}) for EE and 11 cm (16.73 ng μL^{-1}) for DE, the CPM method identified the change in the DNA concentration slope, from a decreasing to a steady trend. For real-time PCR tests, good linear relationships were found between the threshold cycle (Ct) and the initial number of copies ($0.998 \geq R^2 \geq 0.999$). The reaction efficiencies ranged from 95 to 99% for *A. minutum* and from 91.4 to 95.3% for *S. donghaiensis*. To ensure specific amplifications, the melting temperature values (Tm) were systematically checked by analyzing the melting curves. For the *A. minutum* assay, the

standard curve samples as well as the positive samples showed a specific peak at $T_m = 83.05 \pm 0.5^\circ\text{C}$ (see Supplementary Figure 2). In the case of *S. donghaiensis*, the melting curve peak was observed at $T_m = 82.9 \pm 0.5^\circ\text{C}$. Copy numbers <LOQ (= 10 copies/well) for both *A. minutum* and *S. donghaiensis* were observed in some deep sediment layers. In these cases, the target species were considered present in the core layers, but it was not possible to quantify their ITS rDNA copy numbers. The presence of *A. minutum* in deep layers (indicated with star symbols in Figure 3) was confirmed by the sequencing of semi-nested PCR products. Nine and five sequences of 31-45 bp were obtained for DE and EE core layers, respectively. The sequences were aligned with other available sequences (see Supplementary File 1, Supplementary Figure 3) and identified as *A. minutum* at 100% identity (Table 2).

Multidecadal dynamics of Alexandrium minutum and Scrippsiella donghaiensis detected in sediments

Accurate DNA quantification of *A. minutum* ITS1 rDNA copies g^{-1} sediment was obtained from the 10-cm layer (1993 ± 1) to the 1-cm layer (2011 ± 1) of the EE core and from the 22-cm layer (1976 ± 2) to the 1-cm layer (2013 ± 1) of the DE core (Fig. 3), covering a total period of about 40 years. For both EE and DE, in the layers from which quantitative data were obtained, an increasing trend in the concentration of *A. minutum* ITS1 rDNA copies g^{-1} sediment was observed from the bottom to the top layers. This trend was visualized by the moving average calculation (Fig. 3) and statistically confirmed over the period 1989-2014 by the Mann-Kendall test analyses (DE: $\tau = 0.65$, p value = 0.0005; EE: $\tau = 0.911$, p value = 0.0003). In particular, at EE, *A. minutum* ITS1 rDNA copies g^{-1} sediment increased from the 10-cm layer (1993 ± 1 ; 2.72×10^4 copies g^{-1} sediment) to reach a peak at the 1-cm layer (2011 ± 1 ; 4.96×10^7 copies g^{-1} sediment). At DE, ITS1 rDNA copy numbers were higher than at

EE. They increased from the 22-cm layer (1976 ± 2 ; 2.49×10^4 copies g^{-1} sediment), peaking at the 1-cm layer (2013 ± 1 ; 6.73×10^7 copies g^{-1}). ITS1 rDNA copies g^{-1} were slightly correlated with total DNA concentrations in both cores (EE: $R^2 = 0.51$; DE: $R^2 = 0.55$), which were higher in the top than in the bottom layers (see Supplementary Figure 1). In layers from which non-quantitative data were obtained, the presence of *A. minutum* was detected discontinuously, being present along the cores in 5 out of 21 layers and in 9 out of 35 layers for EE and DE, respectively (star symbols in Figure 3). These rDNA traces of *A. minutum* were detected even in the deep sediment layers of both analyzed cores, corresponding to 1939 ± 2 (31 cm) for EE and 1873 ± 6 for DE (57 cm) (Fig. 3).

For *S. donghaiensis*, quantification of ITS1 rDNA copies g^{-1} of sediment was obtained from the 27-cm layer (1952 ± 2) to the 1-cm layer (2011 ± 1) for the EE core, and from the 21-cm layer (1979 ± 2) to the 1-cm layer (2013 ± 1) for the DE core (Fig. 3). The pattern of abundance of ITS rDNA copies observed for *S. donghaiensis* differed from that of *A. minutum* and varied across the sites studied (Fig. 3). At EE, a bimodal pattern of copy number abundance was evident. From the deepest quantifiable 27-cm layer (1952 ± 2 ; 5.1×10^4 copies g^{-1} sediment), the first peak of abundance was evident at the 11-cm layer (1991 ± 1 ; 4.4×10^5 copies g^{-1} sediment) and a second peak corresponding to the highest copy number observed, was found in the top 3 cm (peak of 1.2×10^6 copies g^{-1} sediment at 1 cm (2011 ± 1)). At DE, spikes of abundance were observed at 21 cm (1979 ± 2 ; 1.1×10^5 copies g^{-1} sediment), 13 cm (1995 ± 2 ; 9.13×10^4 copies g^{-1} sediment) and 9 cm (2003 ± 1 ; 1.24×10^5 copies g^{-1} sediment). From the 9-cm layer to the top layer of the DE core, a decrease in copy number abundance was observed (Fig. 3). Over the period 1989-2014, the Mann-Kendall test showed a significant increasing trend in EE ($\tau = 0.601$, p value = 0.0001), but no significant trend was detected in DE ($\tau = -0.295$, p value = 0.0650). The pattern of copies g^{-1} sediment abundance

was slightly correlated with total DNA abundance at EE ($R^2 = 0.53$), but not at DE ($R^2 = 0.01$). *Scrippsiella donghaiensis* was detected up to the bottom layers of both the EE and DE cores (1939 ± 2 and 1866 ± 7 , respectively). In the layers for which non-quantitative data were obtained, the presence of *S. donghaiensis* was detected in 4 out of 4 layers for the EE core and in 16 out of 37 layers for the DE core (Fig. 3).

Multidecadal dynamics of Alexandrium minutum and Scrippsiella donghaiensis in the water column (plankton data)

At the *Lanveoc* station, *A. minutum* concentrations were < 7000 cells L^{-1} until 2012, reaching a peak in July 2014 ($32\,800$ cells L^{-1}). At the *Le Passage* station, regular monitoring activities started when *A. minutum* was first observed in the Bay of Brest in 1990 (<100 cells L^{-1}). From 1992 to 1996, no *A. minutum* cells were detected at the station. From 1997, this species was regularly observed until 2003, but always at low concentrations (<2000 cells L^{-1}). Monitoring in the area stopped in 2003 and was re-established in 2012 when a bloom of $560\,000$ cells L^{-1} occurred on 11th July 2012. No bloom was observed in the area in 2013 but in 2014, *A. minutum* concentrations reached $199\,000$ cells L^{-1} on 7th July. The 2012 bloom at *Le Passage* coincided with a bloom at the *Daoulas* station (42×10^6 cells L^{-1} on 11th July 2012), which represents the highest concentration ever recorded in the bay. Blooms of lower intensity occurred in the following years ($293\,333$ cells L^{-1} in 2013 and $1\,052\,000$ cells L^{-1} in 2014) (see Supplementary Figure 4). A statistically significant increasing trend in *A. minutum* concentrations was depicted by our longer plankton time series at *Le Passage* and *Lanveoc* in the Bay of Brest by the Mann-Kendall test (*Lanveoc*: $\tau = 0.247$, p value = 0.0001; *Le Passage*: $\tau = 0.281$, p value = 0.0050). The *Daoulas* time series was too short (3 years) to analyze a multiannual trend, thus the Mann-Kendall test was not applied. When qualitatively

compared over the overlapping period of analyses, the long-term data series of *A. minutum* obtained from our paleoecological approach (ITS1 rDNA copies g⁻¹ sediment) and from the monitoring activity (plankton data Log(cells L⁻¹) of *Lanveoc* and *Le Passage* stations nicely showed a coherent increasing trend in species abundance from 1990 until 2014 (Fig. 4). For *Scrippsiella* spp., monitoring was carried out uninterruptedly from 1987 until 2000 at *Le Passage*, and from 1995 to 2014 at *Lanveoc*. No monitoring of this taxon has ever been performed at the *Daoulas* station. Lower concentrations of *Scrippsiella* spp. were recorded at *Lanveoc* compared to *Le Passage*. At *Lanveoc*, *Scrippsiella* spp. abundance remained below 8300 cells L⁻¹ until 1998, when it reached 42 000 cells L⁻¹. At *Le Passage*, *Scrippsiella* spp. abundance reached a maximum of 760 000 cells L⁻¹ in 1999. Lower abundances were registered during the following years (see Supplementary Figure 4). At both stations, no trend was detected by the Mann-Kendall coefficient for this taxon (*Lanveoc*: $\tau = -0.02$, p value = 0.5297; *Le Passage*: $\tau = -0.0125$, p value = 0.6773).

Discussion

The paleoecological approach used in this study, based on paleogenetic analyses and ancient cyst revivification, provided historical data on two target dinoflagellate species over a time scale of about 150 years. The focus was mainly on the bloom-forming, toxic species *A. minutum* and then paleogenetic data obtained for the non-toxic species *S. donghaiensis* were used to compare specific ecological patterns. Both species were detected along dated sediment cores, even in deep sediment layers (dating back to 1873 ± 6 for *A. minutum* and 1866 ± 7 for *S. donghaiensis*). Their aDNA concentrations were quantified specifically from 1952 ± 2 or 1976 ± 2 (depending on the species and the cores) using a robust, newly-developed real-time

PCR assay. Moreover, up to 31-34 year-old resting cysts were successfully revived from core sediments.

Real-time PCR and cyst germination

Real-time PCR is a quantitative technique known to be highly sensitive, enabling species abundances to be estimated accurately in different environments even when the DNA target gene copy number is low. The advantage of real-time PCR is the fast processing of a large number of samples compared to cell or cyst counting microscopic procedures, which are time-consuming and often biased by taxonomic identification problems. Several studies have used real-time PCR to quantify the abundance of a large number of toxic phytoplankton species in seawater samples: (*Karenia brevis* (Gray *et al.* 2003); *A. minutum* (Touzet *et al.* 2009; Galluzzi *et al.* 2004); *Alexandrium catenella* (Garneau *et al.* 2011); *Ostreopsis cf. ovata* (Perini *et al.* 2011); *Pseudo-nitzschia* spp. (Fitzpatrick *et al.* 2010); and different diatoms and dinoflagellates (Godhe *et al.* 2008; Murray *et al.* 2011), as well as in superficial sediment samples (Kamikawa *et al.* 2007; Erdner *et al.* 2010).

Real-time PCR was the most appropriate method for our paleogenetic approach, which aimed to detect ancient genetic traces of the presence and abundance of the target species in the Bay of Brest. Yet, when quantifying genetic material in old sediments, DNA degradation is a major issue to be taken into account. Taphonomic processes that may occur in old sediments and the variable preservation conditions of organic matter occurring from one ecosystem to another may influence DNA conservation and thus its quantitative estimation (Boere *et al.* 2011). DNA degradation mostly occurs in very old sediments, such as those that are of thousand years old, and can cause DNA to be fragmented, which can significantly reduce the efficiency of PCR amplification (d'Abbadie *et al.* 2007). The real-time PCR

protocol applied in this study was based on a compromise between i) the best discriminating genetic marker (ITS1 rDNA) for *Scrippsiella* spp. (Gu *et al.* 2008) and *Alexandrium* spp. (John *et al.* 2014), ii) the appropriate length of DNA fragment for real-time PCR assays (100-150 bp) (Arya *et al.* 2005), and iii) the recommended analysis of short DNA fragments (~100-500 bp) in paleogenetic studies (Coolen *et al.* 2013). As the DNA fragments in our samples were relatively recent (about 150 years old) and short (about 100 bp), the degradation and fragmentation issues should theoretically have been minimized. However, given the decreasing DNA concentrations revealed along both sampled cores, a potential degradation of the aDNA analyzed cannot be excluded. The real-time PCR amplifications in sediment did not target DNA exclusively from cysts or cells, therefore the abundance estimations (copies g⁻¹ sediment) cannot be extrapolated in terms of copies per cyst or copies per cell. Furthermore, there is a high inter-and intra-species variability in the rDNA copy number of dinoflagellates. Few studies have estimated the rDNA copy number for protists such as diatoms (61 to 36 896 18S rDNA copies cell⁻¹) and dinoflagellates (1057 to 12 812 18S rDNA copies cell⁻¹) (e.g. Godhe *et al.* (2008)), and the only copy number estimation for *A. minutum* (1084 ± 120.3 copies cell⁻¹) targeted the 5.8S rDNA region (Galluzi *et al.* 2004) and not the ITS1 rDNA region. In fact, it is not certain that the 5.8S and the ITS1 rDNA copy number remained locally relatively constant over time.

Germination of *A. minutum* and *S. donghaiensis* varied between sediment cores. Although real-time PCR analyses revealed the presence of the target species in the oldest sediments, no cyst germination was observed in sediment older than 1981 ± 2 (DE core, 20-cm layer) and 1978 ± 2 (EE core, 17-cm layer). The longest cyst survival time observed in our study was 31-34 years for *S. donghaiensis* (EE core) and 17-19 years for *A. minutum* (DE core). Earlier studies have reported the viability of different dinoflagellate and diatom resting

stages after variable periods of burial in sediments ranging from months to several decades (Lewis *et al.* 1999; McQuoid *et al.* 2002; Mizushima and Matsuoka 2004; Ellegaard *et al.* 2013b), and up to 100 years (Härnström *et al.* 2011; Lundholm *et al.* 2011; Ribeiro *et al.* 2011; Miyazono *et al.* 2012). Assuming that the cyst mandatory dormancy period had passed in our samples, we consider that the unsuccessful germination in old sediment was more likely to be related to cyst viability. Over time, in old sediments, resting stages can undergo diagenetic processes and their survival depends on many physical and chemical conditions in the sediment including oxygen levels, temperature, and pH (Kremp and Anderson 2000). The reconstruction of preservation conditions in old sediments over time is very difficult and it is possible that some physical-chemical processes might have prevented cyst survival in these cores. In addition, although different germination conditions (different media and temperature conditions) were tested and a final optimal combination (temperature, nutrient concentration) was found and systematically applied to all samples, it cannot be excluded that optimal germination conditions vary across sediments of different ages. In fact, *S. donghaiensis* and *A. minutum* are able to germinate over a wide range of environmental conditions (Blanco *et al.* 2009; Gu *et al.* 2008).

Interestingly, germination of *A. minutum* and *S. donghaiensis* was successful only for layers in which aDNA quantification was possible. It can be questioned whether DNA was amplified and quantified mainly from living stocks, represented by resting cysts, from extracellular genetic material or from both. Most DNA in marine sediments has been shown to be extracellular (Dell'Anno and Danovaro 2005) and well preserved from microbial nuclease degradation (Corinaldesi *et al.* 2011), but DNA inside the resting stages of some plankton species is generally thought to be better preserved than extracellular DNA (Boere *et al.* 2011). Real-time PCR data do not distinguish between extracellular and cyst-preserved

genetic material, thus a definitive conclusion regarding the type of DNA quantified in this study is not possible. RNA analysis might have clarified whether active or inactive communities were identified, as explored in Capo *et al.* (2015) where RNA transcripts were found only in the top 2 cm of lacustrine sediments and RNA/DNA analyses showed that genetic material in sediments mainly represented inactive communities. However, RNA analyses and quantitative analyses on cysts were beyond the scope of this study. Our main goal was to obtain historical information about the presence, abundance and viability of *A. minutum* and *S. donghaiensis* in order to depict multidecadal ecological patterns.

Historical records of Alexandrium minutum and Scrippsiella donghaiensis and multiannual dynamics

By means of this paleogenetic approach, the first traces of genetic material of *A. minutum* were detected in the Bay of Brest. Starting from two different cores, it could be inferred that the species was present in the bay considerably earlier than its first description in the Mediterranean Sea in 1960 (Halim 1960), as the first detection of the species in the DE sediment core of the Bay of Brest dated back to 1873 ± 6 . Similarly, using cyst records in dated sediments, Ribeiro *et al.* (2011) established that the dinoflagellate *Gymnodinium catenatum* had been present in the Western Iberian Peninsula since 1889 ± 10 , before its first description documented in 1939 on planktonic viable material. Our data also suggest that the presence of *S. donghaiensis* in the Bay of Brest dated back to 1866 ± 7 , but its formal description is relatively recent (Gu *et al.* 2008) and only a few historical and biogeographical data are available, as the species has only been reported in Australia, Sweden and East China (Gu *et al.* 2008). In fact, *A. minutum* and *S. donghaiensis* could have been present in the bay even before 1873 ± 6 and 1866 ± 7 , respectively. The DE core was not sufficiently long to

highlight the absence of the genetic signal along a consistent number of old sediment layers. Regarding the analyzed cores, the presence of both species was detected irregularly across layers from which data below the limit of quantification were obtained. This could indicate some contamination during the sampling process across the different layers. Yet, our sampling protocol was designed to avoid direct contamination during sampling, both across different layers and with modern DNA (using a clean device for each layer) and along the plastic tube core (collecting only the inner part of each sediment layer). In addition, molecular manipulations in the laboratories were performed following previously developed precautions for paleogenetic analyses to avoid cross-contamination between samples (Anderson-Carpenter *et al.* 2011; Boere *et al.* 2011; Domaizon *et al.* 2013; Gilbert *et al.* 2005). Moreover, similar results were obtained from two different cores, collected and analyzed at two different periods of time. Therefore, we believe that the irregular presence of both species across the two cores is most probably due to the presence of a very small amount of specific genetic material rather than to sample contamination.

In order to validate the multiannual study of species dynamics, the relative species variations in quantitative real-time PCR estimations were compared to those of the plankton time series obtained from monitoring analyses during the overlapping periods of the data series. Previously, real-time PCR has rarely been applied to ancient DNA to compare long-term plankton series and only restrictively to quantify cyanobacteria dynamics in freshwater sediments (Domaizon *et al.* 2013; Martínez de la Escalera *et al.* 2014; Pal *et al.* 2015). To the best of our knowledge, this is the first paleogenetic study carried out in monitored estuarine ecosystems addressing such a comparison between real-time PCR and plankton monitoring data. Interestingly, the statistically significant increase in concentrations of ITS1 rDNA copy number of *A. minutum* depicted from 25 year-old sediment samples of two different cores

corroborate the 24 years of plankton observations carried out at different monitoring stations in the Bay of Brest. When compared qualitatively over the overlapping periods (1989-2014), both the paleogenetic and plankton time data series nicely showed an increasing trend in the concentration of the species *A. minutum* over time (Fig. 4). This trend is particularly evident, and statistically confirmed, from the plankton data of the *Lanveoc* and *Le Passage* stations, which have been followed over the long term, and is also proved by the fact that huge blooms of the species have only recently been observed and monitored in the third station of the bay (*Daoulas*) (Chapelle *et al.* 2015). Conversely, *S. donghaiensis* ITS1 rDNA abundances did not show a coherent pattern and trend between the analyzed cores, suggesting a non-homogenous temporal pattern in the Bay of Brest for this species. The increasing concentration trend depicted for *S. donghaiensis* from paleogenetic data of the EE core was not confirmed by the DE core data, unlike for *A. minutum* for which both the EE and DE paleogenetic data series showed an increase in species concentration. The comparison with plankton data was not possible since *S. donghaiensis* can only be identified genetically (Gu *et al.* 2008) and monitoring data are acquired by optical microscopy analyses, which can only identify genera. Yet, *Scrippsiella* spp. data do not show an increase in the abundance of the taxon and no major bloom of any species of the genus has been registered in the Bay of Brest to date.

Along the Brittany coasts, *A. minutum* has been sporadically observed since 1985, at the very beginning of the REPHY monitoring activities. Today, its ecological success is evident in some areas. For instance, in the Penzé estuary (Bay of Morlaix, north Brittany) this species has produced blooms at more than 10^4 cells L⁻¹ every year for the last 27 years (Dia *et al.* 2014). On the north-western Brittany coast (Aber-Wrac'h), blooms are regularly observed, and in the Bay of Brest, high concentrations of the species have been reported since 2012. Our results show that *A. minutum* was present in the Bay of Brest much earlier than its first

detection by REPHY monitoring. On the basis of these results, we can put forward the hypothesis that *A. minutum* had a long residence period before blooming in the area. The introduction of the species, if any, may have occurred earlier than our first detection of it (1873 ± 6). Future paleoecological reconstruction is required to answer this question over a longer time scale.

Our results demonstrate that the species *A. minutum* has increased greatly in the Bay of Brest in recent years. This could be due to the introduction of a new population, potentially genetically different from original populations, or the natural evolution of the local populations, or the adaptation of the local populations to environmental changes (natural or anthropogenic). In fact, local ecosystem-specific constraints have contributed to shaping the population dynamic of the species *A. minutum* in a shorter period of time in relatively close ecosystems (Dia *et al.* 2014). Since our study was performed only at the species level and not at the population level, it is not possible to evaluate to what extent population introduction, adaptation and evolution contributed to the process of *A. minutum* development in the Bay of Brest. Future paleoecological population-based studies could address the issue of species development over a multidecadal time scale at the intraspecific level, contributing to a better understanding of long-term microbial species phenologies in the marine environment.

Conclusions

This study innovatively associated old-cyst revivification, paleogenetic and plankton-monitoring data to reconstruct the long-term dynamics of two target estuarine dinoflagellate species, *A. minutum* and *S. donghaiensis*. Cyst survival time varied between the target species (31-34 years for *S. donghaiensis* and 17-19 years for *A. minutum*) and, interestingly, was correlated with their quantifiable genetic material. This finding contributes to the debate about

the proportions of intracellular, cyst-protected and extracellular DNA amplifiable from sediments. The paleogenetic data enabled the multidecadal dynamics of the two target species to be studied over a time scale of about 150 years, with quantitative data obtained for about the last 40 years. The most ancient genetic traces found in these two dated core samples suggest that *S. donghaiensis* and *A. minutum* have been present in the Bay of Brest since at least 1866 ± 7 and 1873 ± 6 , respectively. Paleogenetic data clearly showed that *A. minutum* has increased in concentration in recent years, corroborating plankton data over the overlapping period of the two different data series (1989-2014). This study contributes to the development of paleoecological research, showing that this discipline, mostly developed in lacustrine ecosystems to date, can be applied to marine, estuarine ecosystems, providing new perspectives for future research on the biogeography, ecology and evolution of marine microbes.

Funding

This work was financed by the exploratory projects VEHSPA (2012-2013) and KYNDER (2014-2015), supported by the "Laboratoire d'Excellence" LabexMER (*Agence Nationale de la Recherche* (ANR) -10-LABX-19) and co-funded by the French government under the program "*Investissements d'Avenir*", and by the projects of the initiative *ECosphere Continentale et Côtière* (EC2CO) of the *Institut National des Sciences de l'Univers/Centre National de la Recherche Scientifique* (INSU/CNRS): PALMITO (2013-2015), and CA'MOMI (2015-2017), and the ANR HAPAR project (2014-2019). This research was carried out within the framework of K. Klouch's PhD and funded by Ifremer and *Région Bretagne* (Allocation de REcherche Doctorale (ARED) fellowship).

Acknowledgements

The authors wish to thank Xavier Caisey and the other scuba divers from Ifremer for sampling the EE core, and Gwendoline Gregoire and Axel Ehrhold from the laboratory GM/LES of Ifremer for allowing the sampling of the DE in the framework of the project SERABEQ ("Laboratoire d'Excellence" LabexMER (ANR-10-LABX-19)). Pierre Bodenes and Tania Hernández-Fariñas are acknowledged for collaborating in the picture developments and Pascale Malestroit for helping with cyst germination and culture maintenance. Pierre Ramond is acknowledged for helping with statistical tests. Finally, we wish to thank the members of the SG2M/LSEM laboratory of Ifremer for access to their laboratory facilities and for all their technical suggestions. This research falls within the scope of the French GDR (*Groupement de Recherche*) Phycotox (<http://www.phycotox.fr>) (2012-2018) on harmful microalgae and phycotoxins.

Conflict of interest. None declared.

References

- Abdenadher M, Hamza A, Fekih W, *et al.* Factors determining the dynamics of toxic blooms of *Alexandrium minutum* during a 10-year study along the shallow southwestern Mediterranean coasts. *Estuar Coast Shelf Sci* 2012;**106**:102–11.
- Anderson DM, Keafer BA, Kleindinst JL, *et al.* *Alexandrium fundyense* cysts in the Gulf of Maine: long-term time series of abundance and distribution, and linkages to past and future blooms. *Deep Sea Res Part 2 Top Stud Oceanogr* 2014;**103**:6–26.

- Anderson-Carpenter LL, McLachlan JS, Jackson ST, *et al.* Ancient DNA from lake sediments: bridging the gap between paleoecology and genetics. *BMC Evol Biol* 2011;**11**:30.
- Andresen CS, Schmidt S, Seidenkrantz M-S, *et al.* A 100-year record of changes in water renewal rate in Sermilik Fjord and its influence on calving of Helheim Glacier, Southeast Greenland. *Cont Shelf Res* 2014;**85**:21–29.
- Arya M, Shergill IS, Williamson M, *et al.* Basic principles of real-time quantitative PCR. *Expert Rev Mol Diagn* 2005;**5**:1–11.
- Avşar U, Hubert-Ferrari A, De Batist M, *et al.* Sedimentary records of past earthquakes in Boraboy Lake during the last ca 600 years (North Anatolian Fault, Turkey). *Palaeogeogr Palaeoclimatol* 2015;**433**:1–9.
- Bazzoni AM, Caddeo T, Pulina S, *et al.* Spatial distribution and multiannual trends of potentially toxic microalgae in shellfish farms along the Sardinian coast (NW Mediterranean Sea). *Environ Monit Assess* 2015;**187**:86, DOI: 10.1007/s10661-014-4250-3.
- Belin C. Distribution of *Dinophysis* spp. and *Alexandrium minutum* along French coasts since 1984 and their DSP and PSP toxicity levels. In: Smayda TJ, Shimizu Y (eds.). *Toxic Phytoplankton Blooms in the Sea*. Amsterdam: Elsevier, 1993, 469–474.
- Bissett A, Gibson JAE, Jarman SN, *et al.* Isolation, amplification, and identification of ancient copepod DNA from lake sediments. *Limnol Oceanogr-Methods* 2005;**3**:533–42.

- Blanco EP, Lewis J, Aldridge J. The germination characteristics of *Alexandrium minutum* (Dinophyceae), a toxic dinoflagellate from the Fal estuary (UK). *Harmful Algae* 2009;**8**:518–22.
- Boere A, Rijpstra WIC, De Lange GJ, *et al.* Preservation potential of ancient plankton DNA in Pleistocene marine sediments. *Geobiology* 2011;**9**:377–93.
- Capo E, Debroas D, Arnaud F, Domaizon I. Is planktonic diversity well recorded in sedimentary DNA? Toward the reconstruction of past protistan diversity. *Microb Ecol* 2015;**70**:865–75.
- Chang FH, Garthwaite I, Anderson DM, *et al.* Immunofluorescent detection of a PSP-producing dinoflagellate, *Alexandrium minutum*, from Bay of Plenty, New Zealand. *N. Z. J. Mar Freshw Res* 1999; **33**:533– 43.
- Chapelle A, Le Gac M, Labry C, *et al.* The Bay of Brest (France), a new risky site for toxic *Alexandrium minutum* blooms and PSP shellfish contamination. *Harmful Algae News* 2015;**51**:4–5.
- Coolen MJL, Orsi WD, Balkema C, *et al.* Evolution of the plankton paleome in the Black Sea from the Deglacial to Anthropocene. *P Natl Acad Sci USA* 2013;**110**:8609–14.
- Coolen MJL, Overmann J. 217 000-year-old DNA sequences of green sulfur bacteria in Mediterranean sapropels and their implications for the reconstruction of the paleoenvironment. *Envir Microbiol* 2007;**9**:238–49.
- Corinaldesi C, Barucca M, Luna GM, *et al.* Preservation, origin and genetic imprint of extracellular DNA in permanently anoxic deep-sea sediments. *Mol Ecol* 2011;**20**:642–54.

- d'Abbadie, Hofreiter M, Vaisman A, *et al.* Molecular breeding of polymerases for amplification of ancient DNA. *Nat Biotechnol* 2007;**25**:939–43.
- de Vernal A, Eynaud F, Henry M, *et al.* Reconstruction of sea-surface conditions at middle to high latitudes of the Northern Hemisphere during the Last Glacial Maximum (LGM) based on dinoflagellate cyst assemblages. *Quaternary Sci Rev* 2005;**24**:897–924.
- Dell'Anno A, Danovaro R. Extracellular DNA plays a key role in deep-sea ecosystem functioning. *Science* 2005;**309**:2179.
- Dia A, Guillou L, Mauger S, *et al.* Spatiotemporal changes in the genetic diversity of harmful algal blooms caused by the toxic dinoflagellate *Alexandrium minutum*. *Mol Ecol* 2014;**23**: 549–60.
- Domaizon I, Savichtcheva O, Debroas D, *et al.* DNA from lake sediments reveals the long-term dynamics and diversity of *Synechococcus* assemblages. *Biogeosciences* 2013;**10**: 3817–38.
- Durantou L, Rochon A, Ledu D, *et al.* Quantitative reconstruction of sea-surface conditions over the last ~150 years in the Beaufort Sea based on dinoflagellate cyst assemblages: the role of large-scale atmospheric circulation patterns. *Biogeosciences* 2012;**9**:5391-5406.
- Elbrachter M. Exotic flagellates of coastal North Sea waters. *Helgoländer Meeresun* 1999;**52**: 235–42.
- Ellegaard M, Clarke AL, Reuss N, *et al.* Multi-proxy evidence of long-term changes in ecosystem structure in a Danish marine estuary, linked to increased nutrient loading. *Estuar Coast Shelf S* 2006;**68**:567–78.

Ellegaard M, Figueroa RL, Versteegh GJM. Dinoflagellate life cycles, strategy and diversity: key foci for future research. In: Lewis JM, Marret F, Bradley L (eds.). *Biological and Geological Perspectives of Dinoflagellates*. London: The Micropalaeontological Society, Special Publications, Geological Society, 2013a, 249–62.

Ellegaard M, Ribeiro S, Lundholm N, *et al.* Using the sediment archive of living dinoflagellate cysts and other protist resting stages to study temporal population dynamics. In: Lewis JM, Marret F, Bradley L (eds.). *Biological and Geological Perspectives of Dinoflagellates*. London: The Micropalaeontological Society, Special Publications, Geological Society, 2013b, 149–53.

Epp LS, Stoof KR, Trauth MH, *et al.* Historical genetics on a sediment core from a Kenyan lake, intraspecific genotype turnover in a tropical rotifer is related to past environmental changes. *J Paleolimnol* 2010;**43**:939–54.

Erdner DL, Percy L, Keafer B, *et al.* A quantitative real-time PCR assay for the identification and enumeration of *Alexandrium* cysts in marine sediments. *Deep-Sea Res Pt II* 2010;**57**: 279–87.

Fitzpatrick E, Caron DA, Schnetzer A. Development and environmental application of a genus-specific quantitative PCR approach for *Pseudo-nitzschia* species. *Mar Biol* 2010;**157**:1161–69.

Franco JM, Fernandez P, Reguera B. Toxin profiles of natural populations and cultures of *Alexandrium minutum* Halim from Galician (Spain) coastal waters. *J Appl Phycol* 1994;**6**:275–79.

- Galluzzi L, Penna A, Bertozzini E, *et al.* Development of a Real-Time PCR Assay for Rapid Detection and Quantification of *Alexandrium minutum* (a Dinoflagellate). *Appl Environ Microb* 2004;**70**:1199–1206.
- Garneau MÈ, Schnetzer A, Countway PD, *et al.* Examination of the seasonal dynamics of the toxic dinoflagellate *Alexandrium catenella* at Redondo Beach, California, by quantitative PCR. *Appl Environ Microb* 2011;**77**:7669–80.
- Gilbert MTP, Bandelt H-J, Hofreiter M, *et al.* Assessing ancient DNA studies. *Trends Ecol Evol* 2005;**20**:541–44.
- Godhe A, Asplund ME, Härnström K, *et al.* Quantification of diatom and dinoflagellate biomasses in coastal marine seawater samples by real-time PCR. *Appl Environ Microbiol* 2008;**74**:7174–82.
- Godhe A, Otta SK, Rehnstam-Holm AS, *et al.* Polymerase chain reaction in detection of *Gymnodinium mikimotoi* and *Alexandrium minutum* in field samples from southwest India. *Mar Biotechnol* 2001;**3**:152–62.
- Godhe A, Rehnstam-Holm A-S, Karunasagar I, *et al.* PCR detection of dinoflagellate cysts in field sediment samples from tropic and temperate environments. *Harmful Algae* 2002;**1**:361–73.
- Gómez F. Phytoplankton invasions: comments on the validity of categorizing the non-indigenous dinoflagellates and diatoms in European seas. *Mar Poll Bull* 2008;**56**:620–28.

- Gray M, Wawrik B, Paul J, *et al.* Molecular detection and quantitation of the red tide Dinoflagellate *Karenia brevis* in the marine environment. *App Environ Microbiol* 2003;**69**:5726–30.
- Gross J. Re-occurrence of red tide in Cork Harbor, Ireland. *Red Tide Newsletter* 1989;**2**:4–5.
- Gu H, Sun J, Kooistra WHCF, Zeng R. Phylogenetic Position and Morphology of Thecae and Cysts of *Scrippsiella* (Dinophyceae) species in the East China Sea. *J Phycol* 2008;**44**:478–94.
- Guillaud JF, Bouriel L. Relation concentration-débit et évolution temporelle du nitrate dans 25 rivières de la région Bretagne (France). *Rev Sci Eau* 2007;**20** :213–26.
- Halim Y. *Alexandrium minutum*, dinoflagellé provocant des "eaux rouges". *Vie Milieu* 1960;**11**:102–05.
- Hallegraeff G, Steffensen DA, Wetherbee R. Three estuarine Australian dinoflagellates that can produce paralytic shellfish toxins. *J Plankton Res* 1988;**10**:533–41.
- Hansen G, Daugbjerg N, Franco J. Morphology, toxin composition and LSU rDNA phylogeny of *Alexandrium minutum* (Dinophyceae) from Denmark, with some morphological observations on other European strains. *Harmful Algae* 2003;**2**:317–35.
- Härnström K, Ellegaard M, Andersen TJ, *et al.* Hundred years of genetic structure in a sediment revived diatom population. *P Natl Acad Sci USA* 2011;**108**:4252–57.

Hernández-Fariñas T, Soudant D, Barillé L, *et al.* Temporal changes in the phytoplankton community along the French coast of the eastern English Channel and the southern Bight of the North Sea. *ICES J Mar Sci* 2014;**71**:821–833.

Honsell G. First report of *Alexandrium minutum* in northern Adriatic waters (Mediterranean Sea). In: Smayda TJ, Shimizu Y (eds.). *Toxic Phytoplankton Blooms in the Sea*. Amsterdam: Elsevier, 1993, 127–132.

Hou W, Dong H, Li G, *et al.* Identification of photosynthetic plankton communities using sedimentary ancient DNA and their response to late-Holocene climate change on the Tibetan plateau. *Sci Rep* 2014;**4**:6648.

Hwang DF, Lu YH. Influence of environmental and nutritional factors on growth, toxicity, and toxin profile of dinoflagellate *Alexandrium minutum*. *Toxicon* 2000;**38**:1491–1503.

John U, Litaker RW, Montresor M, *et al.* Formal revision of the *Alexandrium tamarense* species complex (Dinophyceae) taxonomy: the introduction of five species with emphasis on molecular-based (rDNA) classification. *Protist* 2014;**165**:779–804.

Kamikawa R, Nagai S, Hosoi-Tanabe S, *et al.* Application of real-time PCR assay for detection and quantification of *Alexandrium tamarense* and *Alexandrium catenella* cysts from marine sediments. *Harmful Algae* 2007;**6**:413–20.

Katsanevakis S, Wallentinus I, Zenetos, *et al.* Impacts of invasive alien marine species on ecosystem services and biodiversity: a pan-European review. *Aquat Invasions* 2014;**9**:391–423.

- Keller MD, Selvin RC, Claus W, *et al.* Media for the culture of oceanic ultraphytoplankton. *J Phycol* 1987;**23**:633–38.
- Kremp A, Anderson DM Factors regulating germination of resting cysts of the spring bloom dinoflagellate *Scrippsiella hangoei* from the northern Baltic Sea. *J Plankton Res* 2000;**22**:1311–1327.
- Laird KR, Fritz SC, Maasch KA, *et al.* Greater drought intensity and frequency before AD 1200 in the Northern Great Plains, USA. *Nature* 1996;**384**:552–55.
- Lejzerowicz, F, Esling P, Majewski W, *et al.* Ancient DNA complements microfossil record in deep-sea subsurface sediments. *Biol Letters* 2013;9:20130283.
- Lewis J, Harris ASD, Jones KJ, *et al.* Long-term survival of marine planktonic diatoms and dinoflagellates in stored sediment samples. *J Plankton Res* 1999;**21**:343–54.
- Lilly EL, Halanych KM, Anderson DM. Phylogeny, biogeography, and species boundaries within the *Alexandrium minutum* group. *Harmful Algae* 2005;**4**:1004–20.
- Liu D, Shen X, Di B, *et al.* Palaeoecological analysis of phytoplankton regime shifts in response to coastal eutrophication. *Mar Ecol-Prog Ser* 2013;**475**:1–14.
- Lundholm N, Clarke AM, Ellegaard M, *et al.* Documenting historical trends in toxic algae: A 100 year-record of changing *Pseudo-nitzschia* species in a sill-fjord related to nutrient loading and temperature. *Harmful Algae* 2010;**9**:449–57.

Martin JL, LeGresley MM, Hanke AR. Thirty years – *Alexandrium fundyense* cyst, bloom dynamics and shellfish toxicity in the Bay of Fundy, eastern Canada. *Deep-Sea Res Pt II* 2014;**103**:27–39.

Martínez de la Escalera, G, Antoniadis D, Bonilla S, *et al.* Application of ancient DNA to the reconstruction of past microbial assemblages and for the detection of toxic cyanobacteria in subtropical freshwater ecosystems. *Mol Ecol* 2014;**23**:5791–802.

McCauley L a. R, Erdner DL, Nagai S, *et al.* Biogeographic analysis of the globally distributed harmful algal bloom species *Alexandrium minutum* (Dinophyceae) based on rRNA gene sequences and microsatellite markers. *J Phycol* 2009;**45**:454–63.

McQuoid MR, Godhe A, Nordberg K. Viability of phytoplankton resting stages in the sediments of a coastal Swedish fjord. *Eur J Phycol* 2002;**37**:191–201.

Mertens KN, Bradley LR, Takano Y, *et al.* Quantitative estimation of Holocene surface salinity variation in the Black Sea using dinoflagellate cyst process length. *Quaternary Sci Rev* 2012;**39**:45–59.

Mertens KN, González C, Delusina I, *et al.* 30 000 years of productivity and salinity variations in the late Quaternary Cariaco Basin revealed by dinoflagellate cysts. *Boreas* 2009;**38**:647–62.

Miyazono A, Nagai S, Kudo I, *et al.* Viability of *Alexandrium tamarense* cysts in the sediment of Funka Bay, Hokkaido, Japan: over a hundred year survival times for cysts. *Harmful Algae* 2012;**16**, 81–88.

- Mizushima K, Matsuoka K. Vertical distribution and germination ability of *Alexandrium* spp. cysts (Dinophyceae) in the sediments collected from Kure Bay of the Seto Inland Sea, Japan. *Phycol Res* 2004;**52**:408–13.
- Mousing EA, Andersen TJ, Ellegaard M. Changes in the abundance and species composition of phytoplankton in the last 150 years in the southern Black Sea. *Estuaries Coasts* 2013;**36**:1206–18.
- Murray S, Wiese M, Stüken A, *et al.* sxtA-based quantitative molecular assay to identify saxitoxin-producing harmful algal blooms in marine waters. *App Environ Microbiol* 2011;**77**:7050–57.
- Nehring S. Non-indigenous phytoplankton species in the North Sea: supposed region of origin and possible transport vector. *Arch Fish Mar Res* 1998;**46**:181–94.
- Pal S, Gregory-Eaves I, Pick FR. Temporal trends in cyanobacteria revealed through DNA and pigment analyses of temperate lake sediment cores. *J Paleolimnol* 2015;**54**:87–101.
- Panieri G, Lugli S, Manzi V, *et al.* Ribosomal RNA gene fragments from fossilized cyanobacteria identified in primary gypsum from the late Miocene, Italy. *Geobiology* 2010;**8**:101–11.
- Penna A, Battocchi C, Garcés E, *et al.* Detection of microalgal resting cysts in European coastal sediments using a PCR-based assay. *Deep Sea Res Part II* 2010;**57**:288–300.
- Perini F, Casabianca A, Battocchi C, *et al.* New approach using the real-time PCR method for estimation of the toxic marine dinoflagellate *Ostreopsis* cf. *ovata* in marine environment. *PloS One* 2011;**6**:1–9.

- Persson A, Godhe A, Karlson B. Dinoflagellate cysts in recent sediments from the west coast of Sweden. *Bot Mar* 2000;**43** 69–79.
- Pietramellara G, Ascher J, Borgogni F, *et al.* Extracellular DNA in soil and sediment: fate and ecological relevance. *Biol Fert Soils* 2009;**45**:219–35.
- Pospelova V, Price AM, Pedersen TF. Palynological evidence for late Quaternary climate and marine primary productivity changes along the California margin. *Paleoceanography* 2015;**30**:1–18.
- Probert I, Siano, R, Poirier C, *et al.* *Brandtodinium* gen. nov. and *B. nutricula* comb. Nov. (Dinophyceae), a dinoflagellate commonly found in symbiosis with polycystine radiolarians. *J Phycol* 2014;**50**:388–99.
- R Core Team. R: A language and environment for statistical computing. R Foundation for Statistical Computing. Vienna, Austria. 2015. <https://www.R-project.org/>.
- Rawlence NJ, Lowe DJ, Wood JR, *et al.* Using palaeoenvironmental DNA to reconstruct past environments: progress and prospects. *J Quat Sci* 2014;**29**:610–26.
- Ribeiro S, Amorim A, Andersen TJ. Reconstructing the history of an invasion: the toxic phytoplankton species *Gymnodinium catenatum* in the Northeast Atlantic. *Biol Invasions* 2011;**14**:969–85.
- Ribeiro S, Terje B, Lundholm N, Ellegaard M. Hundred years of environmental change and phytoplankton ecophysiological variability archived in coastal sediments. *PloS One* 2013;**8**:1–8.

- Rozen S, Skaletsky H. Primer3 on the WWW for general users and for biologist programmers. In: Krawetz S, Misener S (eds.). *Bioinformatics Methods and Protocols: Methods in Molecular Biology*. Totowa, NJ, USA, Humana Press, 2000, 365-86.
- Saari HK, Schmidt S, Castaing P, *et al.* The particulate $^7\text{Be}/^{210}\text{Pb}_{\text{xs}}$ and $^{234}\text{Th}/^{210}\text{Pb}_{\text{xs}}$ activity ratios as tracers for tidal-to-seasonal particle dynamics in the Gironde estuary (France): Implications for the budget of particle-associated contaminants. *Sci Total Environ* 2010;**408**:4784–94.
- Schmidt S, De Deckker P. Present-day sedimentation rates on the southern and southeastern Australian continental margins. *Aust J of Earth Sci* 2015;**62**:143–50.
- Schmidt S, Jouanneau J-M, Weber O, *et al.* Sedimentary processes in the Thau Lagoon (South France): from seasonal to century time scales. *Estuar Coast Shelf Sci* 2007; **72**: 534–42.
- Shuler AJ, Paternoster J, Brim M, *et al.* Spatial and temporal trends of the toxic diatom *Pseudo-nitzschia* in the Southeastern Atlantic United States. *Harmful Algae* 2012;**17**:6–13.
- Stoof-Leichsenring KR, Epp LS, Trauth MH, *et al.* Hidden diversity in diatoms of Kenyan Lake Naivasha: a genetic approach detects temporal variation. *Mol Ecol* 2012;**21**:1918–30.
- Taylor WA. Change-Point Analysis: A powerful new tool for detecting changes, <http://www.variation.com/cpa/tech/changepoint.html>, 2000.
- Theroux S, D'Andrea WJ, Toney J, *et al.* Phylogenetic diversity and evolutionary relatedness of alkenone-producing haptophyte algae in lakes, implications for continental paleotemperature reconstructions. *Earth Planet Sci Lett* 2010;**300**:311–20.

Touzet N, Keady E, Raine R, *et al.* Evaluation of taxa-specific real-time PCR, whole-cell FISH and morphotaxonomy analyses for the detection and quantification of the toxic microalgae *Alexandrium minutum* (Dinophyceae), Global Clade ribotype. *FEMS Microbiol Ecol* 2009;**67**:329–41.

Touzet N, Lacaze J, Maher M, *et al.* Summer dynamics of *Alexandrium ostenfeldii* (Dinophyceae) and spirolide toxins in Cork Harbour, Ireland. *Mar Ecol Progr Ser* 2011;**425**:21–33.

Usup G, Pin LC, Ahmad A. *Alexandrium* (Dinophyceae) species in Malaysian waters. *Harmful Algae* 2002;**1**:265–75.

Verleye TG, Mertens K, Louwye S, *et al.* Holocene salinity changes in the southwestern Black Sea: a reconstruction based on dinoflagellate cysts. *Palynology* 2009;**33**:77–100.

Weckström J, Korhola A, Erästö P, *et al.* Temperature patterns over the past eight centuries in Northern Fennoscandia inferred from sedimentary diatoms. *Quaternary Res* 2006;**66**: 78–86.

Yu S-Y, Berglund BE. A dinoflagellate cyst record of Holocene climate and hydrological changes along the southeastern Swedish Baltic coast. *Quaternary Res* 2007;**67**: 215–24.

Yue S, Pilon P, Cavadias G. Power of the Mann-Kendall and Spearman's rho tests for detecting monotonic trends in hydrological series *J Hydrol* 2002;**259**:254–71.

Zonneveld KAF, Chen L, Elshanawany R, *et al.* The use of dinoflagellate cysts to separate human-induced from natural variability in the trophic state of the Po River discharge plume over the last two centuries. *Mar Poll Bull* 2012;**64**:114–32.

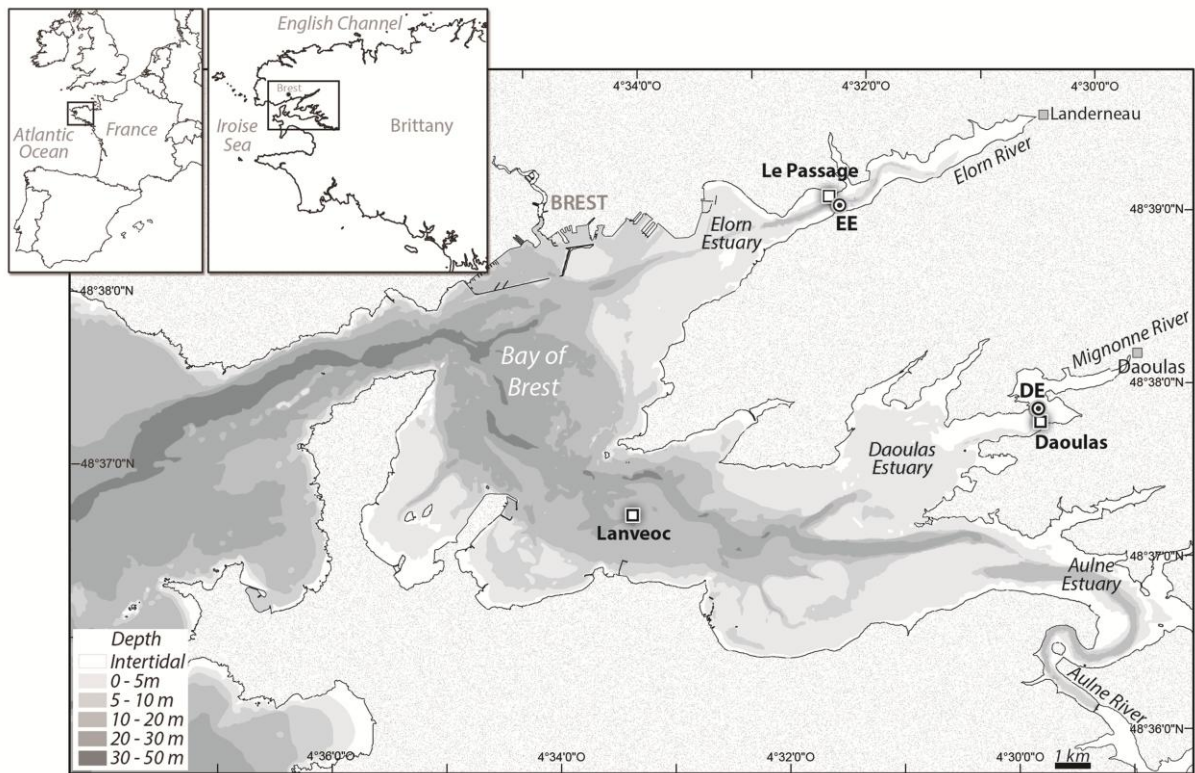


Figure 1. Map of the Bay of Brest with the core sampling sites (Elorn Estuary: EE; Daoulas Estuary: DE), and the monitored plankton stations (*Le Passage*, *Daoulas*, *Lanveoc*).

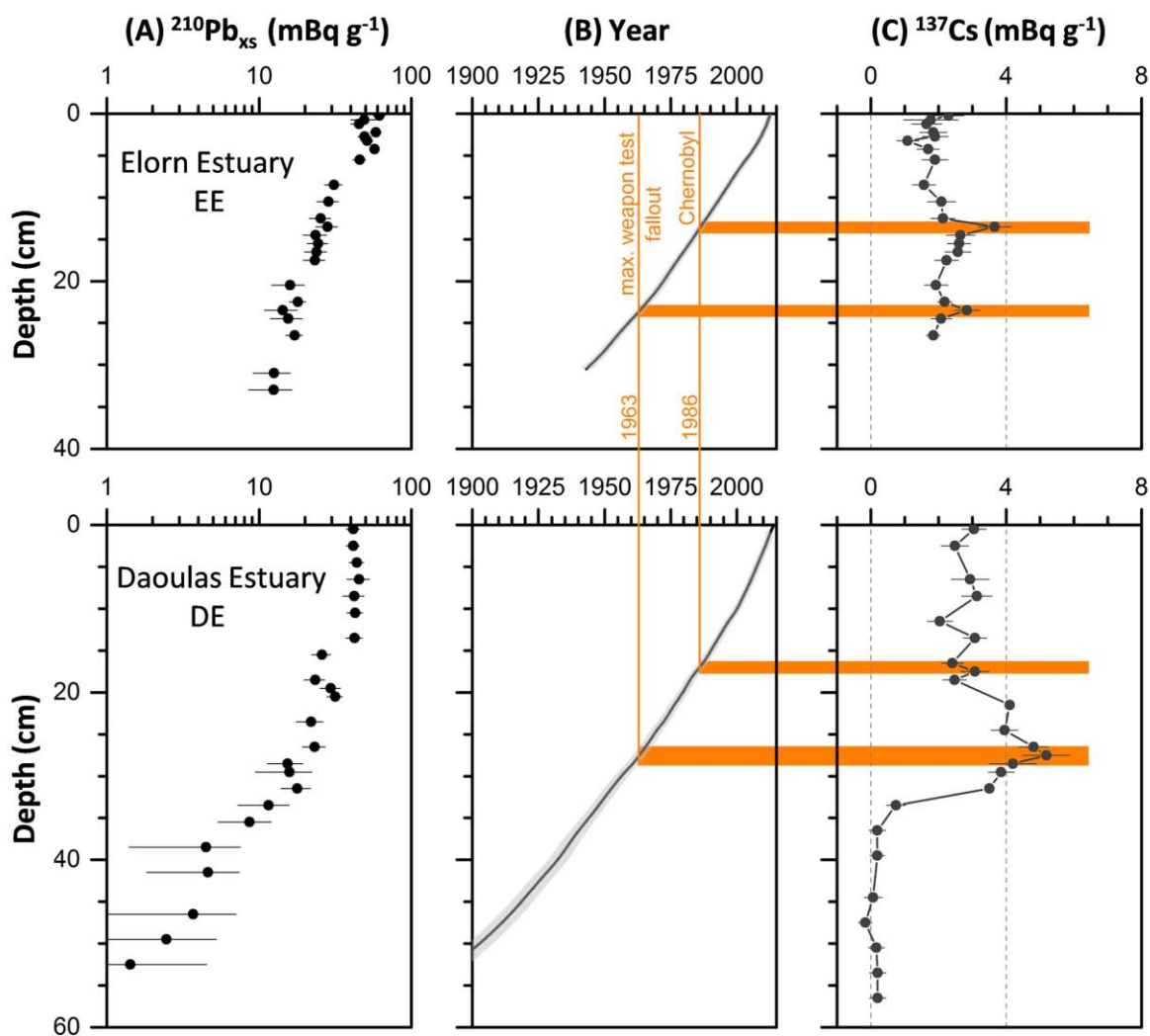


Figure 2. $^{210}\text{Pb}_{\text{xs}}$ profile (A), ages of sedimentary layers, based on CSR model (B) and ^{137}Cs profile (C) with depth along the cores in the Elorn (EE, upper panel) and Daoulas (DE, lower panel) estuaries.

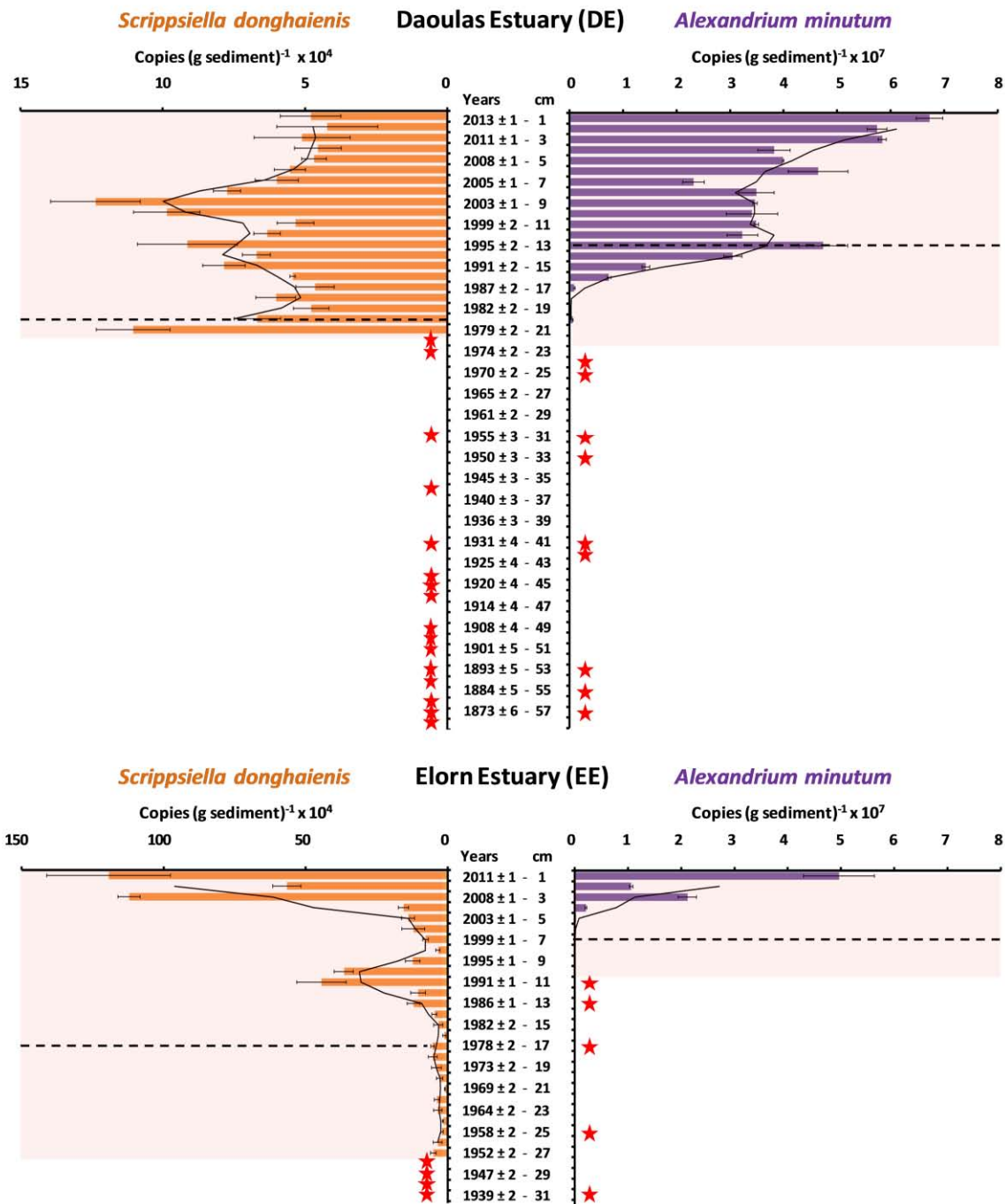


Figure 3. ITS1 rDNA copies g⁻¹ sediment for *Scrippsiella donghaiensis* (orange) and *Alexandrium minutum* (purple) estimated by real-time PCR in Daoulas (DE) and Elorn (EE) estuaries. Colored shadows indicate the layers for which reliable ITS1 rDNA quantifications were obtained. Stars indicate the layers where the presence of the species was detected but quantitative data were below the limit of quantification of our real-time PCR assays. The dashed lines indicate the limit layer of respective species germination. The black curves represent calculated moving average on the quantitative data.

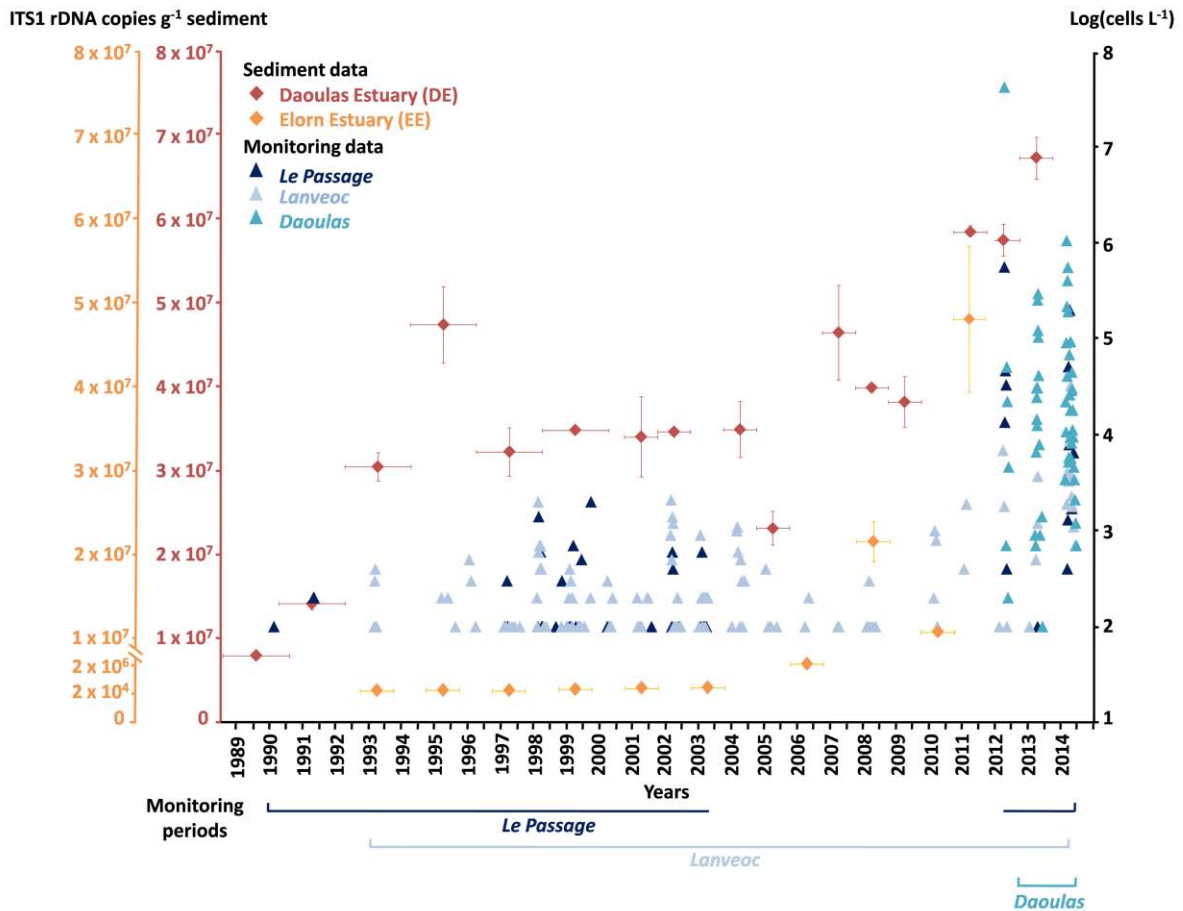


Figure 4. Comparison of paleogenetic and plankton data (REPHY) for *Alexandrium minutum* in the Bay of Brest for the overlapping period of the time series (1989-2014). Copy numbers of ITS1 rDNA g⁻¹ sediment of the DE (red diamonds; red scale) and EE (orange diamonds; orange scale) data series are plotted with their standard deviation error bars (vertical bars). Horizontal bars represent error on sediment dating. All cell concentration data ≥ 100 cells L⁻¹ gathered at the three monitoring stations (*Le Passage*, *Lanveoc*, *Daoulas*) are expressed in Log(cells L⁻¹) (triangles with different blue tones) during the monitored periods (horizontal colored lines).

Table 1. Primer sets designed to target the ITS1 rDNA region of *Alexandrium minutum* and *Scrippsiella donghaiensis* by the different PCR amplification methods.

| Target species | Genetic region | PCR method | Primer sets | Primer sequences Forward (5'-3') Reverse (5'-3') | Amplicon size (bp) |
|----------------------------------|----------------|-------------|--------------------|--|--------------------|
| <i>Alexandrium minutum</i> | ITS1 | Real-time | Am_48F Am_148 R | TGAGCTGTGGTGGGGTTCC GGTCATCAACACAGCAGCA | 100 |
| <i>Alexandrium minutum</i> | ITS1 | Semi-nested | Am_55F Am_148 R | TGGTGGGGTTCCTAGGCT GGTCATCAACACAGCAGCA | 93 |
| <i>Scrippsiella donghaiensis</i> | ITS1 | Real-time | SD_357F SD_468R | TATTCTGGCAACACCTTCCAC AGATGCTTAGCAAGTTGAGCG | 110 |

Table 2. *Alexandrium minutum* semi-nested PCR sequences obtained from DE and EE cores with their respective GenBank accession numbers.

| Species | Core ID | Sediment layers (cm) | Sediment layer dating | Semi-nested sequences (5'-3') |
|----------------------------|---------|----------------------|-----------------------|--|
| <i>Alexandrium minutum</i> | DE | 24 | 1972 ± 2 | ATGGCTTGCTTCTGCAAGCGCTTTCATGCTGCTGTGTTGAT |
| <i>Alexandrium minutum</i> | DE | 25 | 1970 ± 2 | GGCTTGCTTCTGCAAGCGCTTTCATGCTGCTGTGTTGAT |
| <i>Alexandrium minutum</i> | DE | 31 | 1955 ± 3 | GGCATGGCTTGCTTCTGCAAGCGCTTTCATGCTGCTGTGTTGAT |
| <i>Alexandrium minutum</i> | DE | 33 | 1950 ± 3 | GGCATGGCTTGCTTCTGCAAGCGCTTTCATGCTGCTGTGTTGAT |
| <i>Alexandrium minutum</i> | DE | 41 | 1931 ± 4 | ATGGCTTGCTTCTGCAAGCGCTTTCATGCTGCTGTGTTGAT |
| <i>Alexandrium minutum</i> | DE | 42 | 1928 ± 4 | GGCATGGCTTGCTTCTGCAAGCGCTTTCATGCTGCTGTGTTGAT |
| <i>Alexandrium minutum</i> | DE | 53 | 1893 ± 5 | GGCATGGCTTGCTTCTGCAAGCGCTTTCATGCTGCTGTGTTGAT |
| <i>Alexandrium minutum</i> | DE | 54 | 1889 ± 5 | GGCATGGCTTGCTTCTGCAAGCGCTTTCATGCTGCTGTGTTGAT |
| <i>Alexandrium minutum</i> | DE | 57 | 1873 ± 6 | GGCATGGCTTGCTTCTGCAAGCGCTTTCATG |
| <i>Alexandrium minutum</i> | EE | 11 | 1991 ± 1 | CATGGCTTGCTTCTGCAAGCGCTTTCATGCTGCTGTGTTGAT |
| <i>Alexandrium minutum</i> | EE | 13 | 1986 ± 1 | GGCATGGCTTGCTTCTGCAAGCGCTTTCATGCTGCTGTGTTGAT |
| <i>Alexandrium minutum</i> | EE | 17 | 1978 ± 2 | GCATGGCTTGCTTCTGCAAGCGCTTTCATGCTGCTGTGTTGAT |
| <i>Alexandrium minutum</i> | EE | 25 | 1958 ± 2 | GGCATGGCTTGCTTCTGCAAGCGCTTTCATGCTGCTGTGTTGAT |
| <i>Alexandrium minutum</i> | EE | 31 | 1939 ± 2 | GGCTTGCTTCTGCAAGCGCTTTCATGCTGCTGTGTTGAT |

Table 3. *Scrippsiella* spp. strains obtained from the Elorn Estuary (EE) and Daoulas Estuary (DE) dated sediment layers with their respective Genbank accession number and Roscoff culture collection (RCC) number.

| Species | Strain ID | Core sediment layer (cm) | Sediment layer dating | GenBank accession number | RCC ID |
|----------------------------------|--------------|--------------------------|-----------------------|--------------------------|--------|
| <i>Scrippsiella donghaiensis</i> | IFR-SDO-Sc34 | EE2 | 2010 ± 1 | KX009607 | 4711 |
| <i>Scrippsiella donghaiensis</i> | IFR-SDO-Sc35 | EE2 | 2010 ± 1 | KX009606 | 4712 |
| <i>Scrippsiella donghaiensis</i> | IFR-SDO-Sc38 | EE4 | 2006 ± 1 | KX009603 | 4713 |
| <i>Scrippsiella donghaiensis</i> | IFR-SDO-Sc39 | EE4 | 2006 ± 1 | KX009602 | 4714 |
| <i>Scrippsiella donghaiensis</i> | IFR-SDO-Sc40 | EE4 | 2006 ± 1 | KX009601 | - |
| <i>Scrippsiella donghaiensis</i> | IFR-SDO-Sc22 | EE9 | 1995 ± 1 | KX009619 | - |
| <i>Scrippsiella donghaiensis</i> | IFR-SDO-Sc23 | EE9 | 1995 ± 1 | KX009618 | - |
| <i>Scrippsiella donghaiensis</i> | IFR-SDO-Sc24 | EE9 | 1995 ± 1 | KX009617 | 4715 |
| <i>Scrippsiella donghaiensis</i> | IFR-SDO-Sc25 | EE9 | 1995 ± 1 | KX009616 | 4716 |
| <i>Scrippsiella donghaiensis</i> | IFR-SDO-Sc26 | EE9 | 1995 ± 1 | KX009615 | - |
| <i>Scrippsiella donghaiensis</i> | IFR-SDO-Sc51 | EE10 | 1993 ± 1 | KX009592 | 4717 |
| <i>Scrippsiella donghaiensis</i> | IFR-SDO-Sc53 | EE10 | 1993 ± 1 | KX009591 | 4718 |
| <i>Scrippsiella donghaiensis</i> | IFR-SDO-Sc54 | EE10 | 1993 ± 1 | KX009590 | - |
| <i>Scrippsiella donghaiensis</i> | IFR-SDO-Sc1 | EE11 | 1991 ± 1 | KX009637 | - |
| <i>Scrippsiella donghaiensis</i> | IFR-SDO-Sc2 | EE11 | 1991 ± 1 | KX009636 | 4733 |
| <i>Scrippsiella donghaiensis</i> | IFR-SDO-Sc3 | EE11 | 1991 ± 1 | KX009635 | - |
| <i>Scrippsiella donghaiensis</i> | IFR-SDO-Sc4 | EE11 | 1991 ± 1 | KX009634 | - |
| <i>Scrippsiella donghaiensis</i> | IFR-SDO-Sc5 | EE11 | 1991 ± 1 | KX009638 | - |
| <i>Scrippsiella donghaiensis</i> | IFR-SDO-Sc6 | EE11 | 1991 ± 1 | KX009639 | - |
| <i>Scrippsiella donghaiensis</i> | IFR-SDO-Sc7 | EE11 | 1991 ± 1 | KX009640 | - |
| <i>Scrippsiella donghaiensis</i> | IFR-SDO-Sc55 | EE12 | 1989 ± 2 | KX009589 | - |
| <i>Scrippsiella donghaiensis</i> | IFR-SDO-Sc57 | EE12 | 1989 ± 2 | KX009588 | - |
| <i>Scrippsiella donghaiensis</i> | IFR-SDO-Sc8 | EE13 | 1986 ± 2 | KX009633 | - |
| <i>Scrippsiella donghaiensis</i> | IFR-SDO-Sc9 | EE13 | 1986 ± 2 | KX009632 | - |
| <i>Scrippsiella donghaiensis</i> | IFR-SDO-Sc10 | EE13 | 1986 ± 2 | KX009631 | 4719 |
| <i>Scrippsiella donghaiensis</i> | IFR-SDO-Sc11 | EE13 | 1986 ± 2 | KX009630 | - |
| <i>Scrippsiella donghaiensis</i> | IFR-SDO-Sc12 | EE13 | 1986 ± 2 | KX009629 | - |
| <i>Scrippsiella donghaiensis</i> | IFR-SDO-Sc13 | EE13 | 1986 ± 2 | KX009628 | 4720 |
| <i>Scrippsiella donghaiensis</i> | IFR-SDO-Sc14 | EE13 | 1986 ± 2 | KX009627 | 4721 |
| <i>Scrippsiella donghaiensis</i> | IFR-SDO-Sc15 | EE13 | 1986 ± 2 | KX009626 | 4734 |
| <i>Scrippsiella donghaiensis</i> | IFR-SDO-Sc16 | EE13 | 1986 ± 2 | KX009625 | - |
| <i>Scrippsiella donghaiensis</i> | IFR-SDO-Sc17 | EE13 | 1986 ± 2 | KX009624 | - |
| <i>Scrippsiella donghaiensis</i> | IFR-SDO-Sc18 | EE13 | 1986 ± 2 | KX009623 | - |
| <i>Scrippsiella donghaiensis</i> | IFR-SDO-Sc19 | EE13 | 1986 ± 2 | KX009622 | - |
| <i>Scrippsiella donghaiensis</i> | IFR-SDO-Sc20 | EE13 | 1986 ± 2 | KX009621 | 4722 |
| <i>Scrippsiella donghaiensis</i> | IFR-SDO-Sc21 | EE13 | 1986 ± 2 | KX009620 | - |
| <i>Scrippsiella donghaiensis</i> | IFR-SDO-Sc58 | EE14 | 1984 ± 2 | KX009587 | 4730 |
| <i>Scrippsiella donghaiensis</i> | IFR-SDO-Sc59 | EE14 | 1984 ± 2 | KX009586 | - |
| <i>Scrippsiella donghaiensis</i> | IFR-SDO-Sc60 | EE14 | 1984 ± 2 | KX009585 | 4731 |
| <i>Scrippsiella donghaiensis</i> | IFR-SDO-Sc61 | EE14 | 1984 ± 2 | KX009584 | - |
| <i>Scrippsiella donghaiensis</i> | IFR-SDO-Sc27 | EE17 | 1978 ± 2 | KX009614 | 4723 |
| <i>Scrippsiella donghaiensis</i> | IFR-SDO-Sc28 | EE17 | 1978 ± 2 | KX009613 | 4724 |
| <i>Scrippsiella donghaiensis</i> | IFR-SDO-Sc29 | EE17 | 1978 ± 2 | KX009612 | 4725 |
| <i>Scrippsiella donghaiensis</i> | IFR-SDO-Sc30 | EE17 | 1978 ± 2 | KX009611 | - |
| <i>Scrippsiella donghaiensis</i> | IFR-SDO-Sc31 | EE17 | 1978 ± 2 | KX009610 | 4726 |
| <i>Scrippsiella trochoidea</i> | IFR-STR-Sc36 | EE4 | 2006 ± 1 | KX009605 | - |

| | | | | | |
|----------------------------------|--------------|------|----------|----------|------|
| <i>Scrippsiella trochoidea</i> | IFR-STR-Sc37 | EE4 | 2006 ± 1 | KX009604 | 4732 |
| <i>Scrippsiella trochoidea</i> | IFR-STR-Sc41 | EE4 | 2006 ± 1 | KX009600 | - |
| <i>Scrippsiella trochoidea</i> | IFR-STR-Sc42 | EE4 | 2006 ± 1 | KX009599 | 4727 |
| <i>Scrippsiella trochoidea</i> | IFR-STR-Sc43 | EE4 | 2006 ± 1 | KX009598 | - |
| <i>Scrippsiella trochoidea</i> | IFR-STR-Sc45 | EE4 | 2006 ± 1 | KX009597 | 4728 |
| <i>Scrippsiella trochoidea</i> | IFR-STR-Sc32 | EE5 | 2003 ± 1 | KX009609 | - |
| <i>Scrippsiella trochoidea</i> | IFR-STR-Sc33 | EE5 | 2003 ± 1 | KX009608 | - |
| <i>Scrippsiella trochoidea</i> | IFR-STR-Sc46 | EE6 | 2001 ± 1 | KX009596 | - |
| <i>Scrippsiella trochoidea</i> | IFR-STR-Sc47 | EE6 | 2001 ± 1 | KX009595 | - |
| <i>Scrippsiella trochoidea</i> | IFR-STR-Sc48 | EE8 | 1997 ± 1 | KX009594 | - |
| <i>Scrippsiella trochoidea</i> | IFR-STR-Sc49 | EE8 | 1997 ± 1 | KX009593 | 4729 |
| <i>Scrippsiella donghaiensis</i> | IFR-SDO-S5 | DE17 | 1987 ± 2 | KX009641 | 4735 |
| <i>Scrippsiella donghaiensis</i> | IFR-SDO-S8 | DE19 | 1982 ± 2 | KX009642 | 4736 |
| <i>Scrippsiella donghaiensis</i> | IFR-SDO-S7 | DE20 | 1981 ± 2 | KX009643 | 4737 |
| <i>Scrippsiella trochoidea</i> | IFR-STR-S2 | DE10 | 2001 ± 1 | KX009644 | 4738 |
| <i>Scrippsiella trochoidea</i> | IFR-STR-S3 | DE13 | 1995 ± 2 | KX009645 | 4739 |
| <i>Scrippsiella trochoidea</i> | IFR-STR-S9 | DE15 | 1991 ± 2 | KX009646 | 4740 |
| <i>Scrippsiella trochoidea</i> | IFR-STR-S4 | DE17 | 1987 ± 2 | KX009647 | 4741 |
| <i>Scrippsiella trochoidea</i> | IFR-STR-S6 | DE17 | 1987 ± 2 | KX009648 | 4742 |